

# Auger Generation as an Intrinsic Limit to Tunneling Field-Effect Transistor Performance

**Jamie T. Teherani**

Assistant Professor

Department of Electrical Engineering

Columbia University

[j.teherani@columbia.edu](mailto:j.teherani@columbia.edu)

Based on Teherani et al.,

*Journal of Applied Physics*, 2016

<http://dx.doi.org/10.1063/1.4960571>



COLUMBIA | ENGINEERING

The Fu Foundation School of Engineering and Applied Science

# Collaborators

**Sapan Agarwal**

Sandia National Laboratories

**Winston Chern, Dimitri Antoniadis**

Massachusetts Institute of Technology

**Paul Solomon**

IBM T.J. Watson Research Center

**Eli Yablonovitch**

University of California, Berkeley

NSF Center for Energy Efficient Electronics Science (E3S)

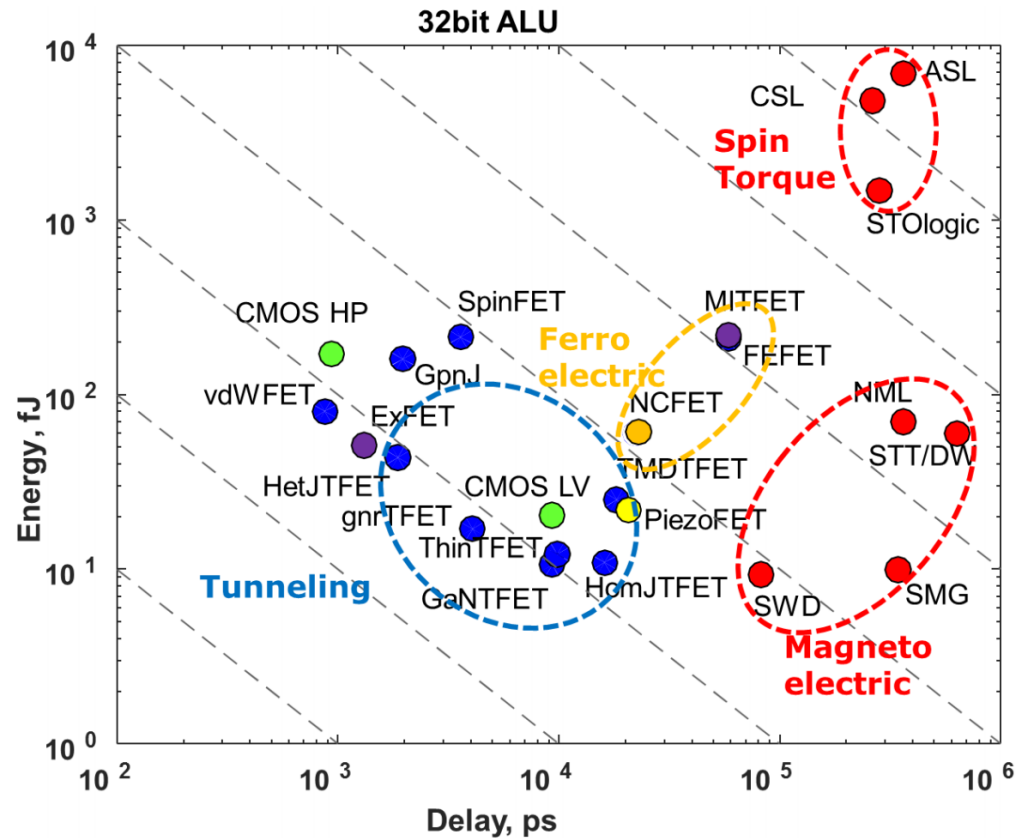


# Outline

- Why TFETs?
- Brief Introduction to TFETs
- State-of-the-Field for TFETs
- Auger Generation
- Rate Equation
- Comparison to BTBT
- Commentary

# Why TFETs?

- One of the most *promising* beyond-CMOS devices

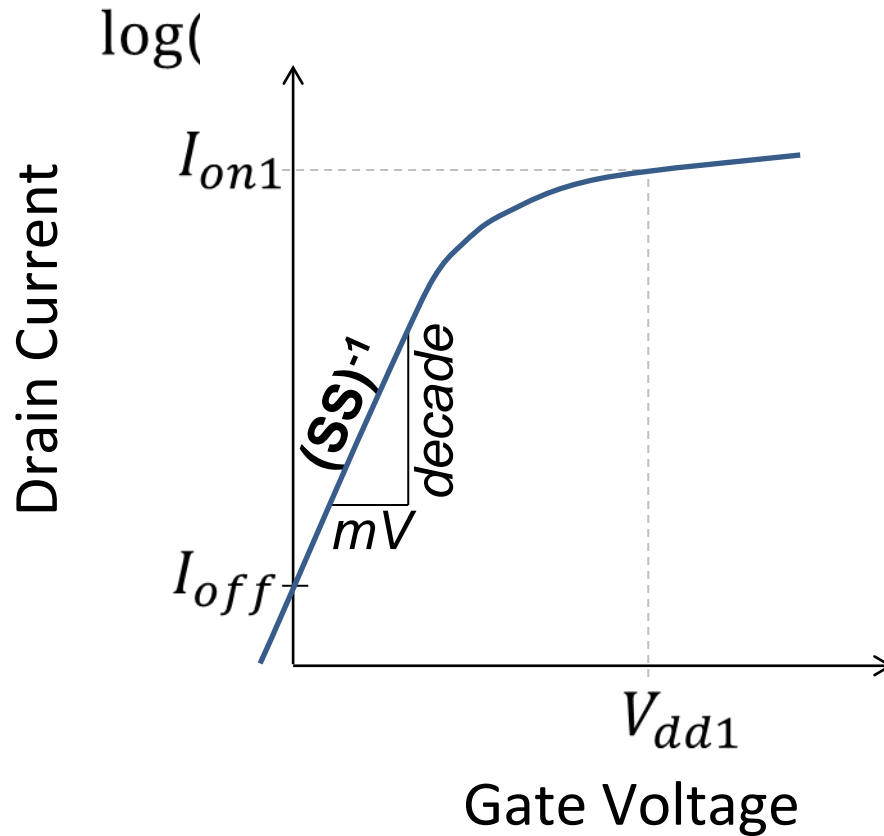


- Key potential advantages
  - looks like a MOSFET
  - drop-in replacement to existing CMOS productions lines
  - small energy-delay product

## **Brief Introduction to TFETs**

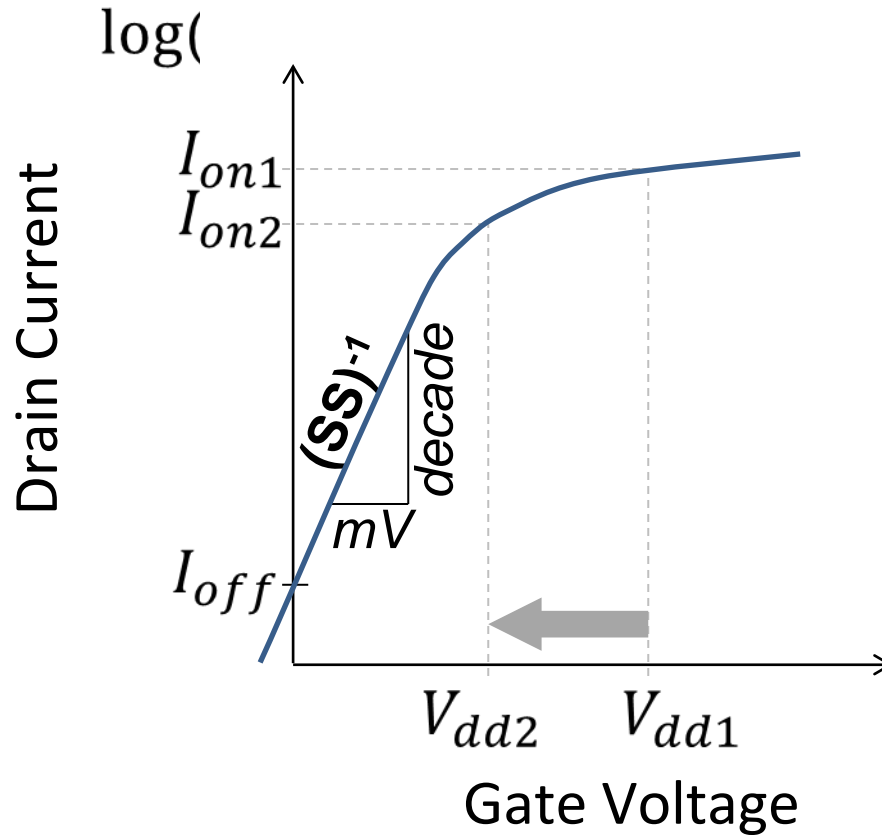
To explain TFETs, let's begin with MOSFETs

# Transfer characteristics for a MOSFET



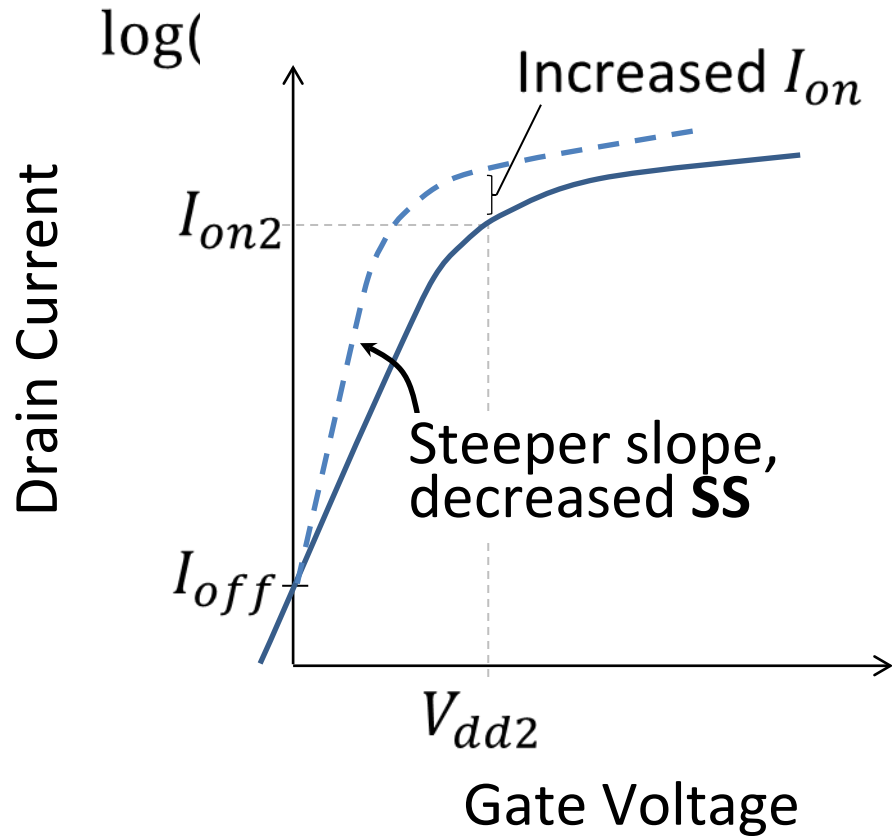
**SS**—subthreshold swing (mV/decade)

# Reducing the voltage reduces the output current and switching speed



**SS**—subthreshold swing (mV/decade)

Decreasing the SS gives improved performance at a lower voltage

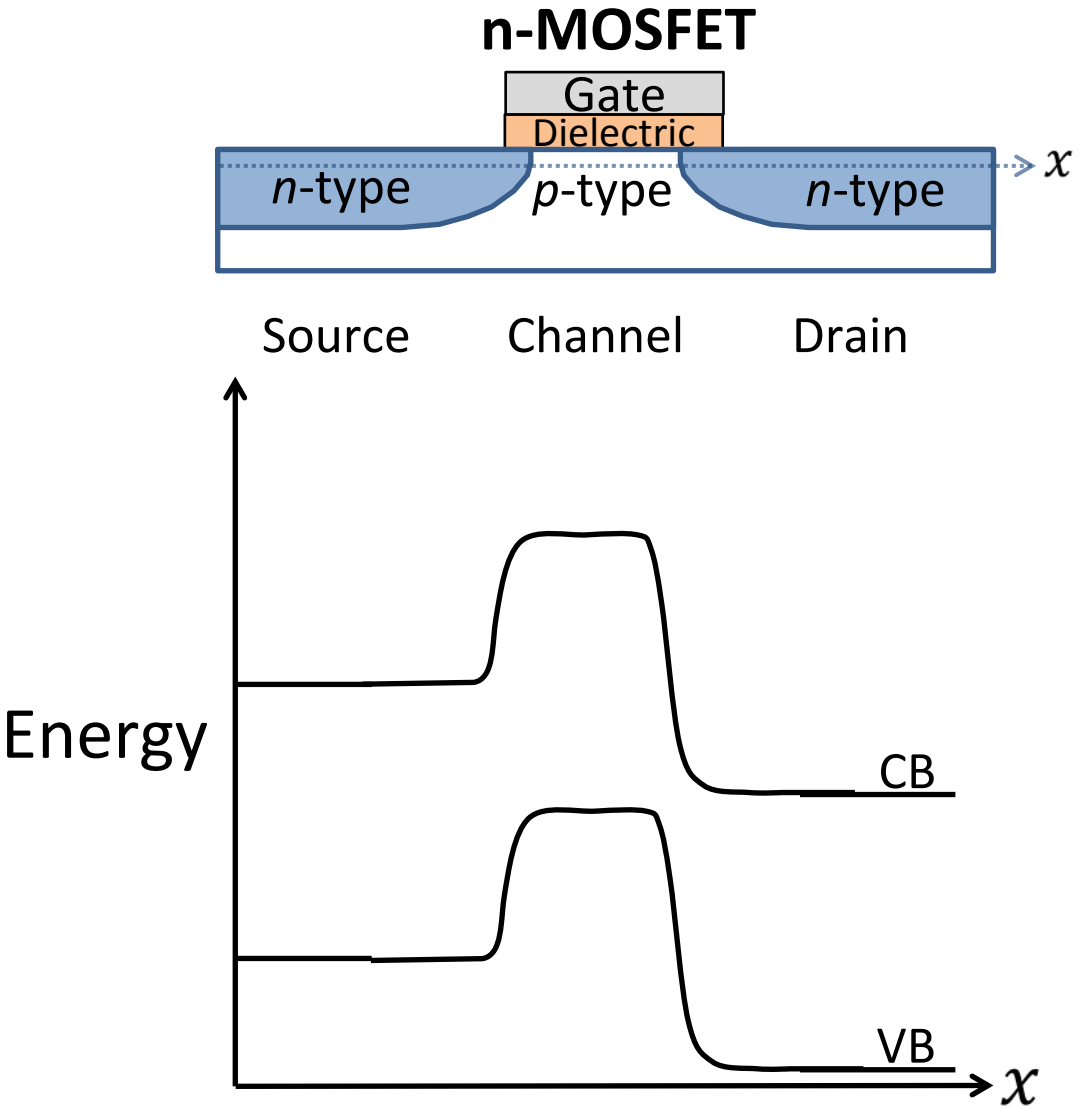


**SS**—subthreshold swing (mV/decade)

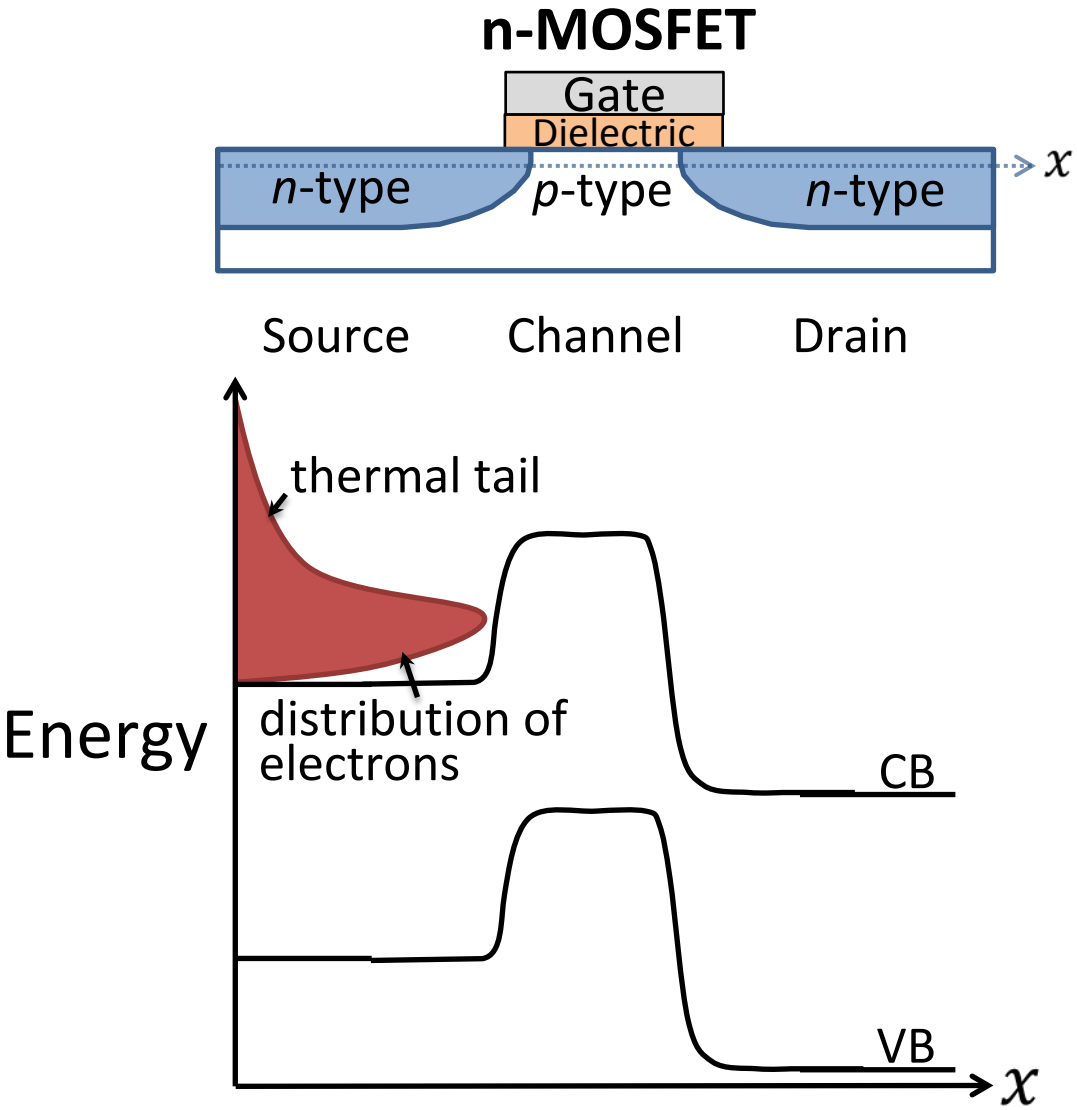


What limits the SS in MOSFETs?

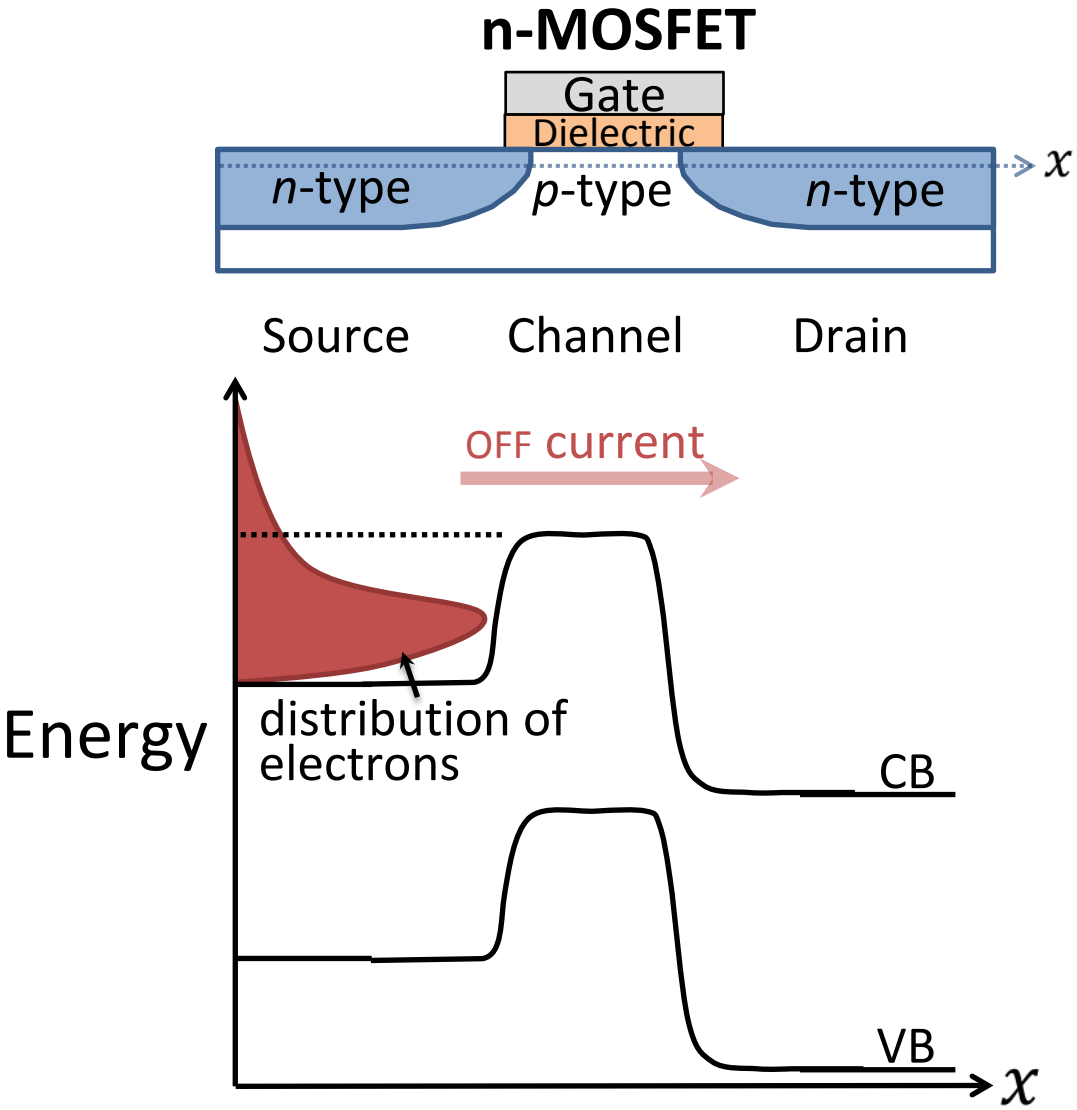
# Band diagram for a MOSFET in the OFF-state



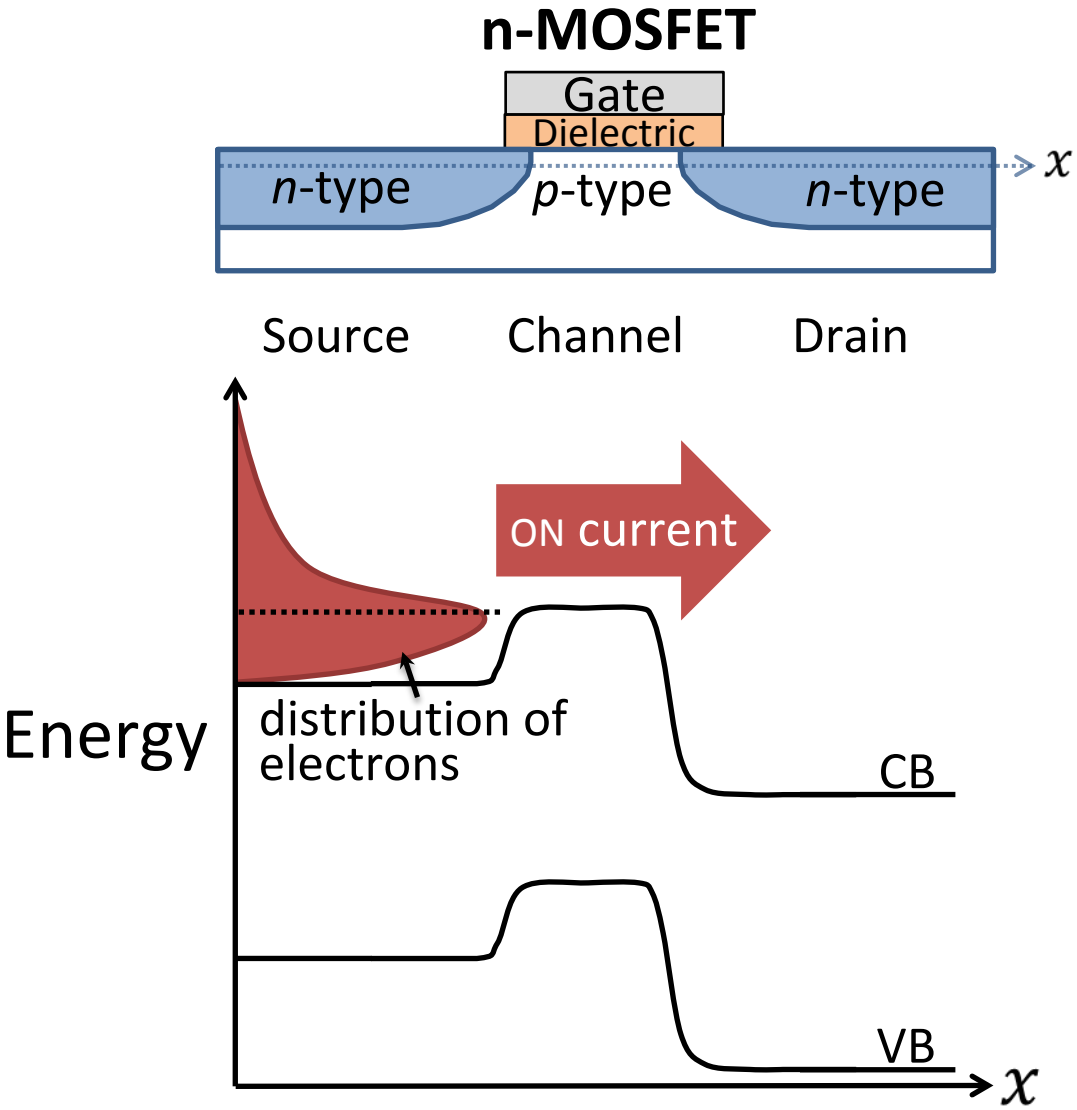
# A thermal distribution of electrons exist in the source



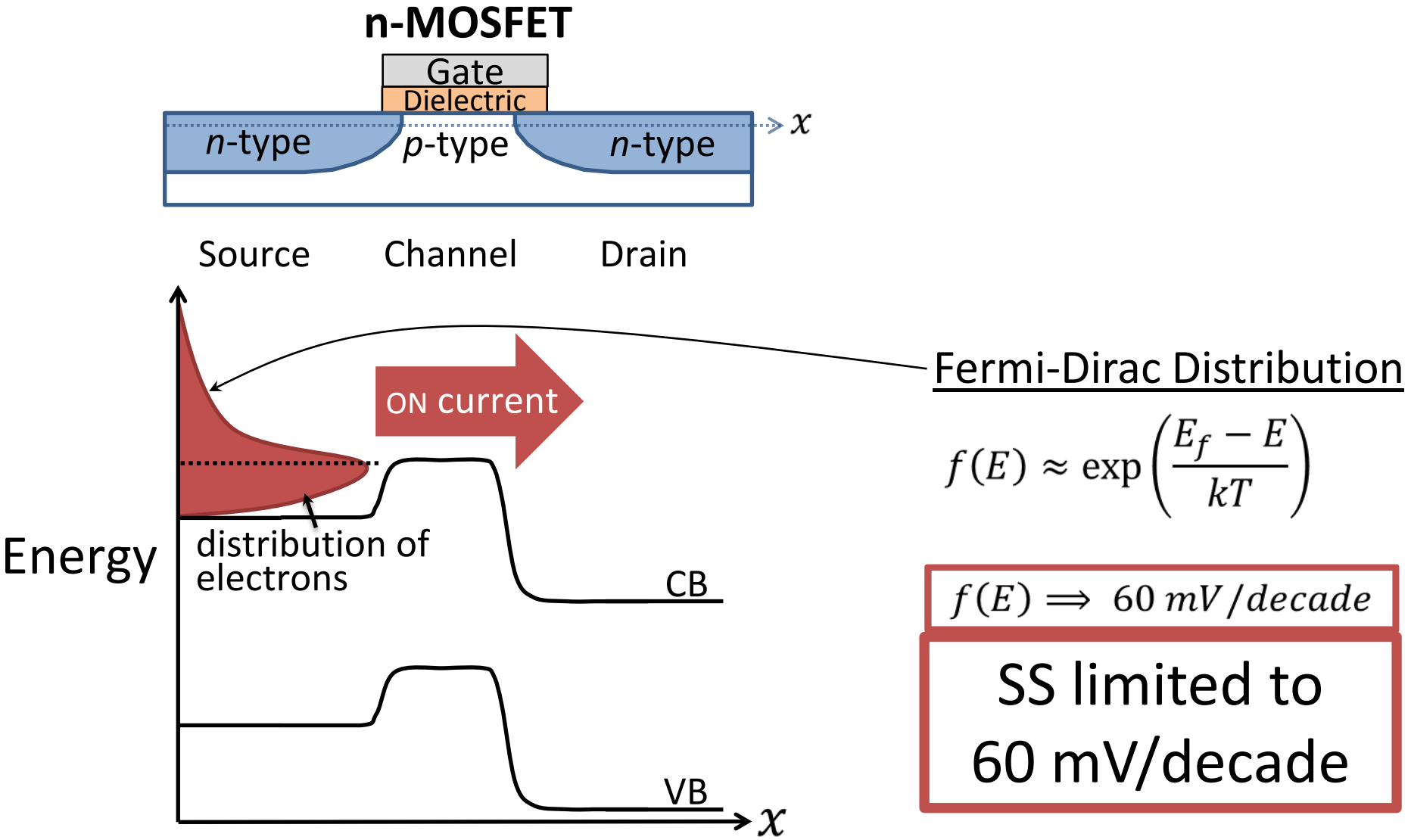
# OFF current is limited by a thermal tail of electrons



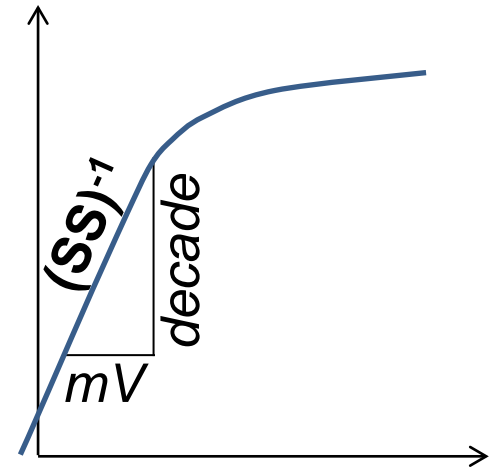
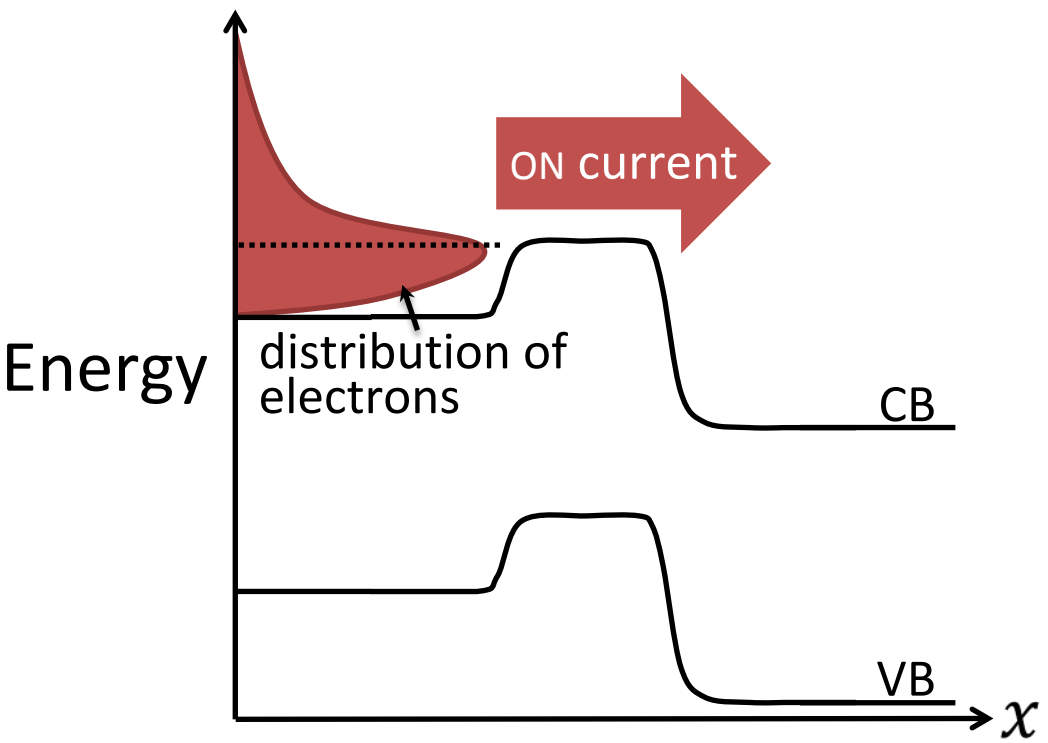
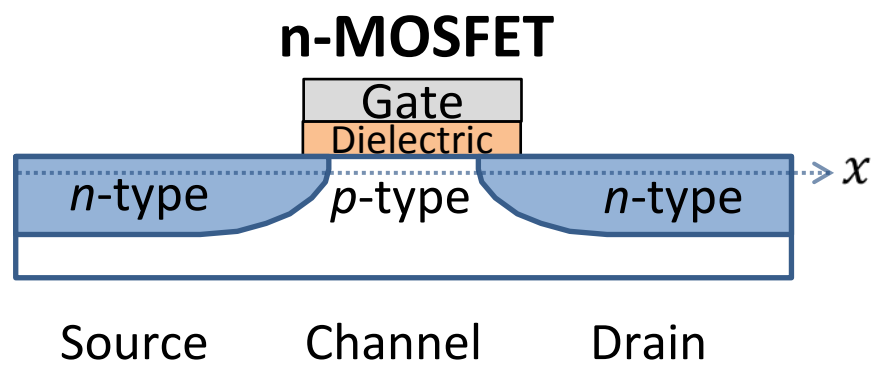
# Gate bias lowers the barrier for electrons and current increases



# SS in a MOSFET is limited to 60 mV/decade



# SS in a MOSFET is limited to 60 mV/decade



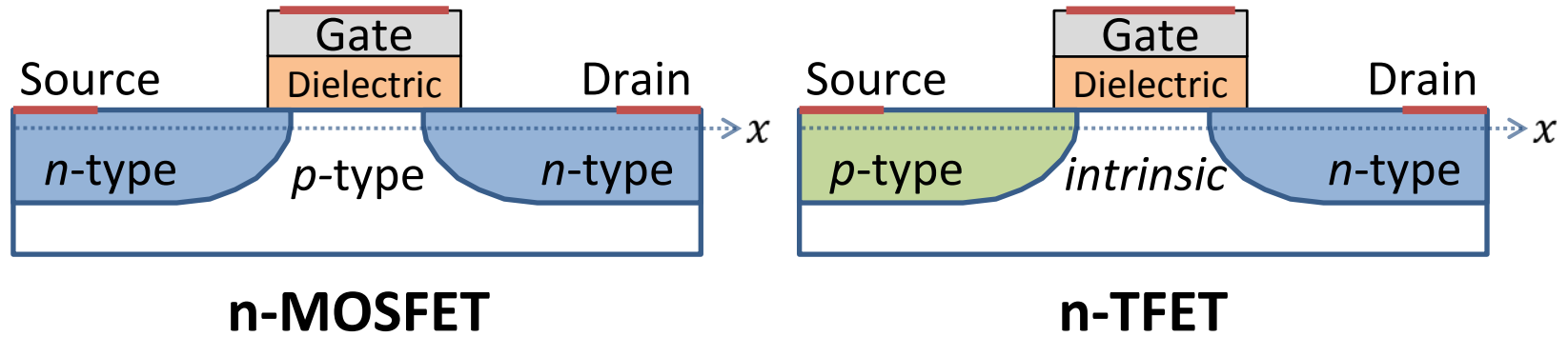
## Fermi-Dirac Distribution

$$f(E) \approx \exp\left(\frac{E_f - E}{kT}\right)$$

$$f(E) \Rightarrow 60 \text{ mV/decade}$$

**SS limited to  
60 mV/decade**

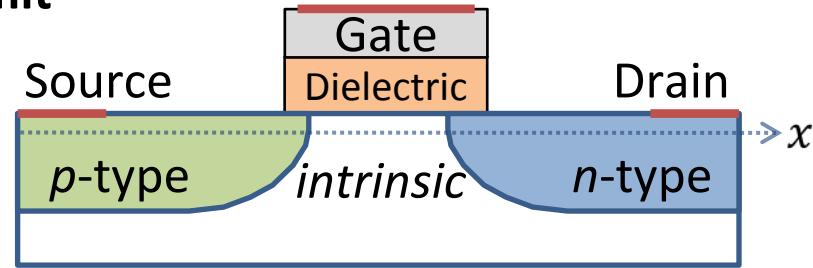
# TFET structure is similar to a MOSFET



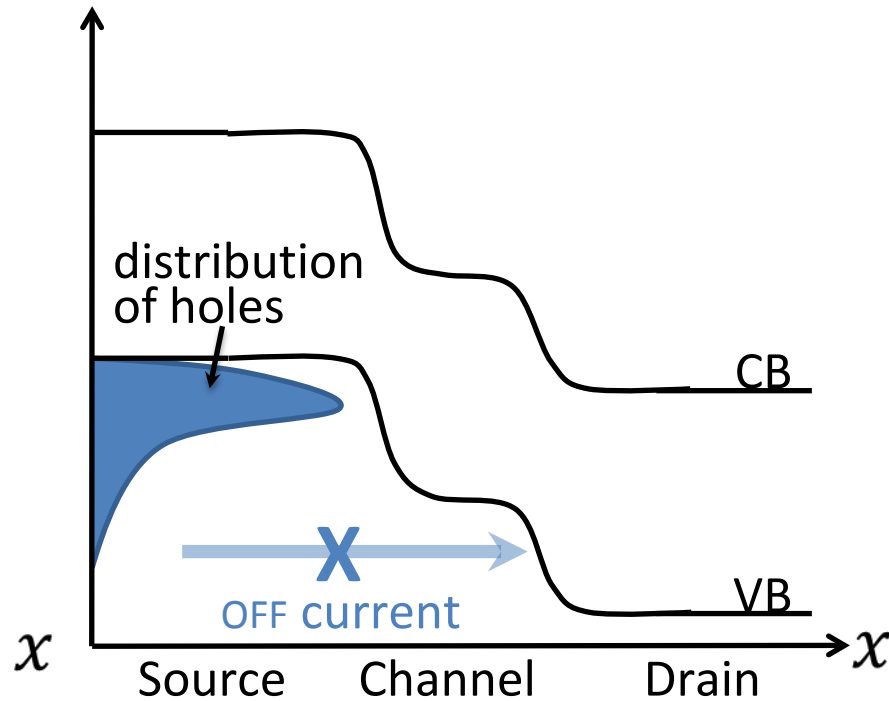


# TFET design prevents OFF current from thermal tail

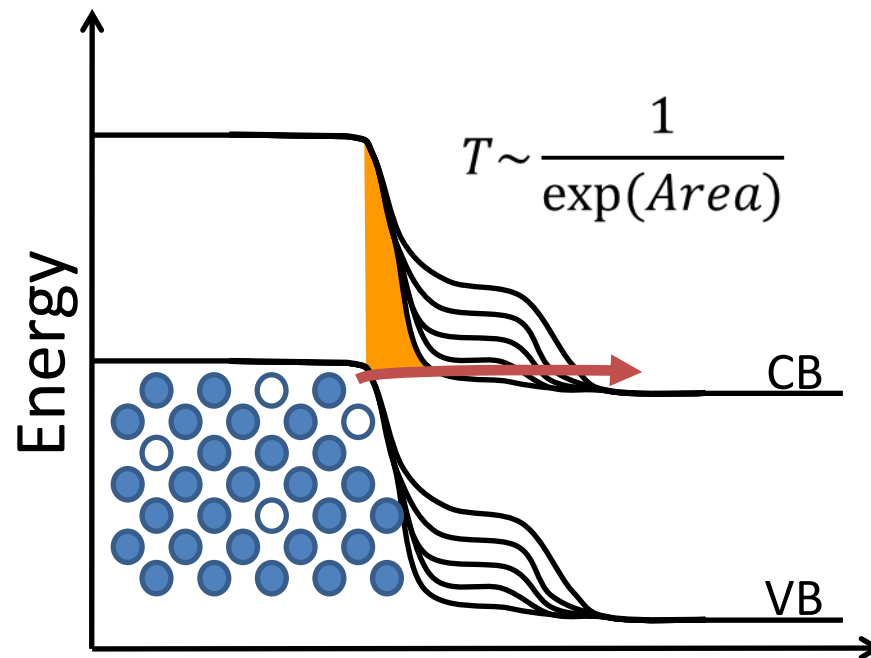
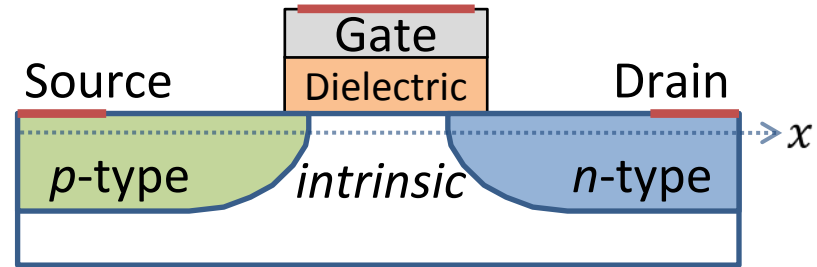
→ no 60 mV/decade limit



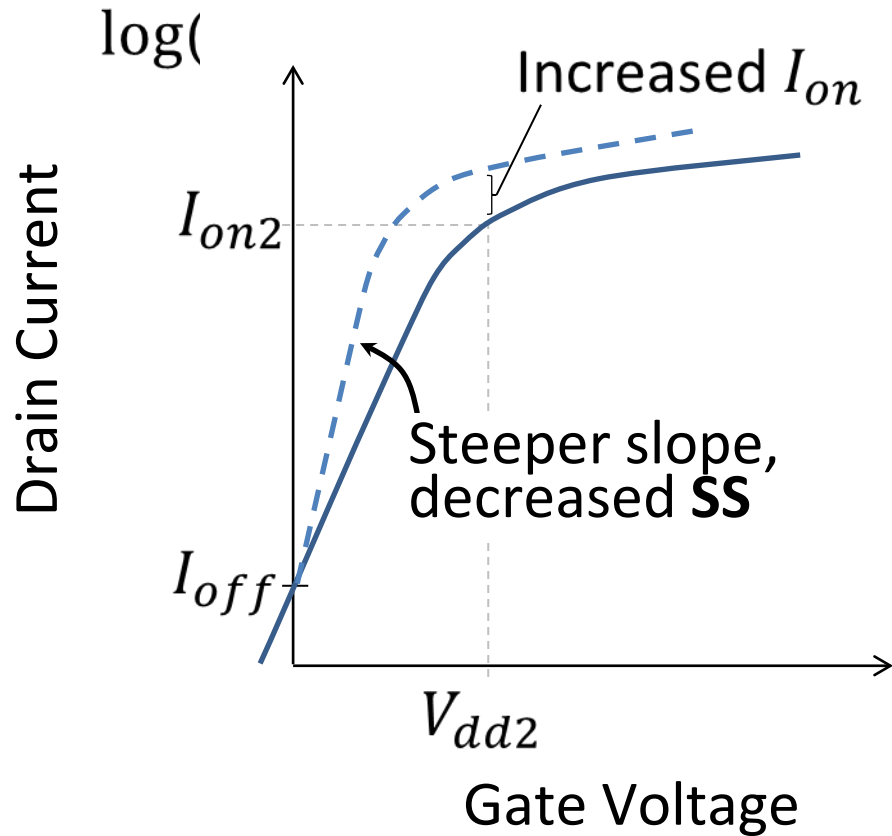
**n-TFET**



# TFETs turn-on by modulating the tunneling path



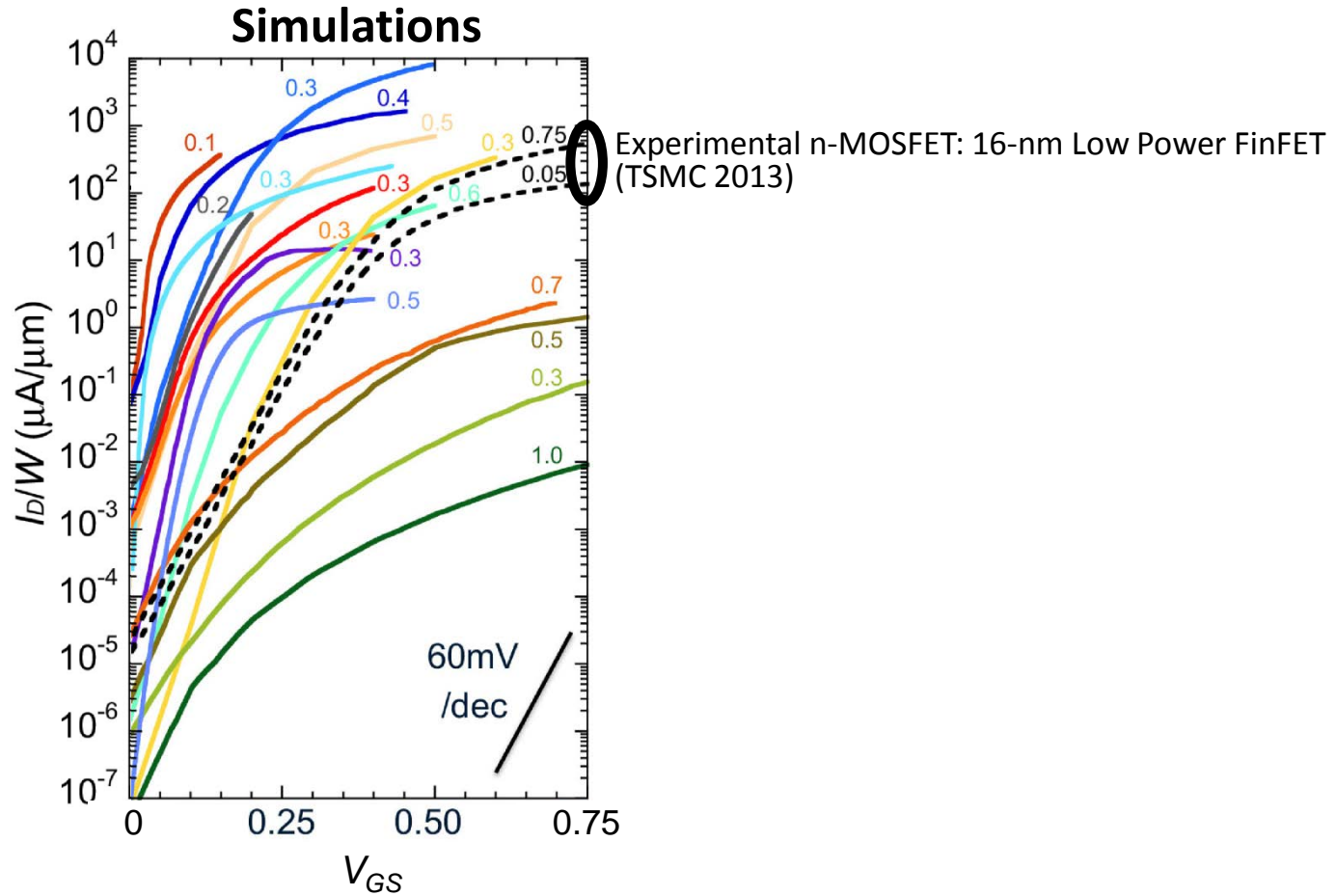
Since TFETs are governed by different device physics, SS can be  $< 60$  mV/decade



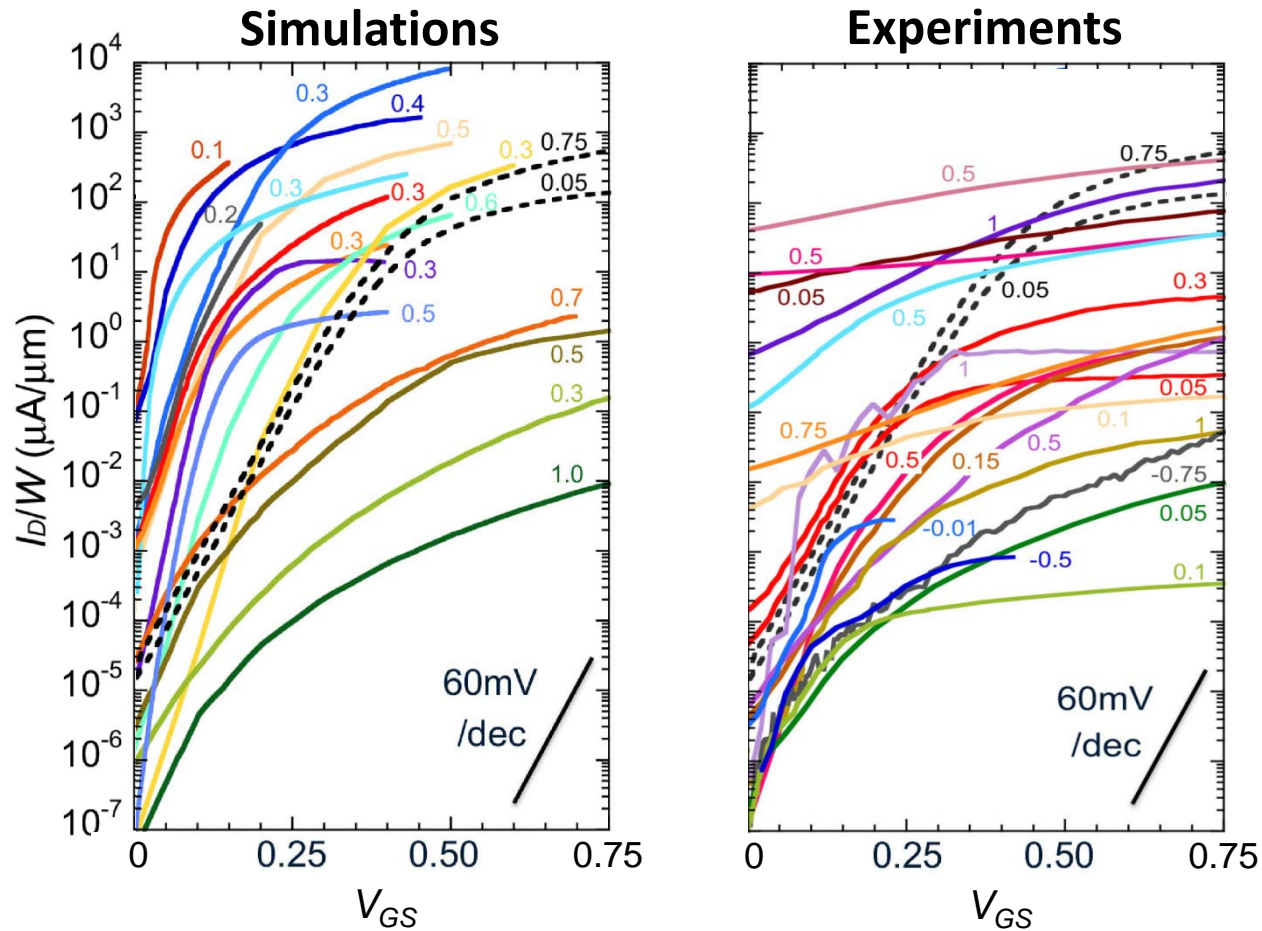
**SS**—subthreshold swing (mV/decade)

# State-of-the-Field for TFETs

# TFET simulations suggest superior results



# Many TFET simulations are in sharp contrast to experimental results



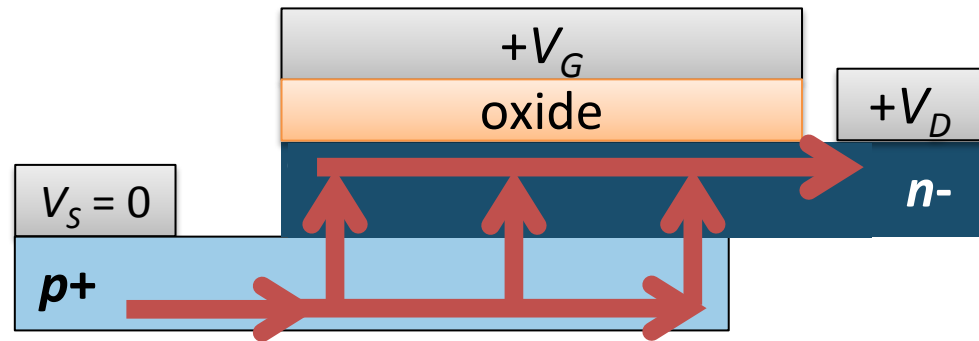
Traps and defects are certainly a big concern...

*My question:*

**Are there intrinsic mechanisms that limit TFET performance?**

# We'll study an ideal TFET:

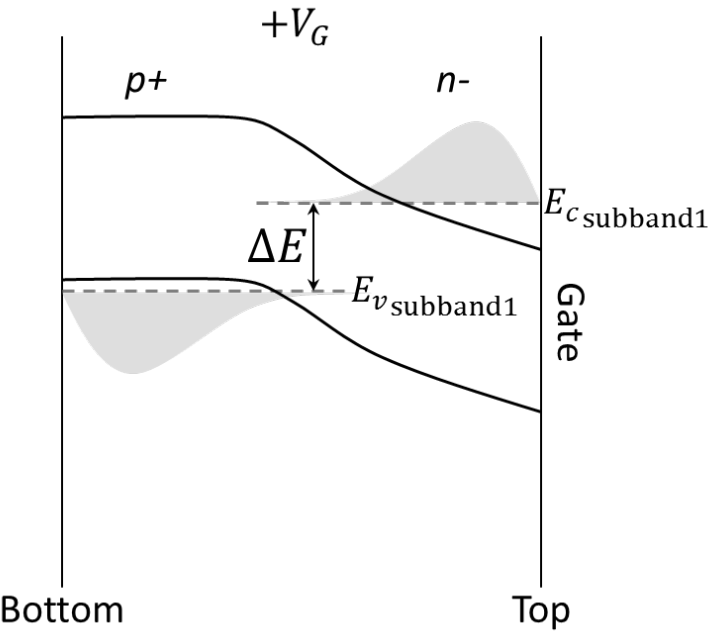
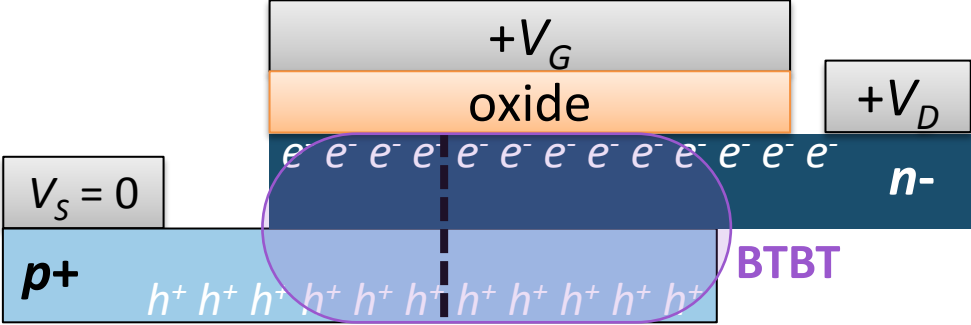
- “Perpendicular TFET”
- “Line TFET”
- “In-line TFET”
- “Vertical TFET”



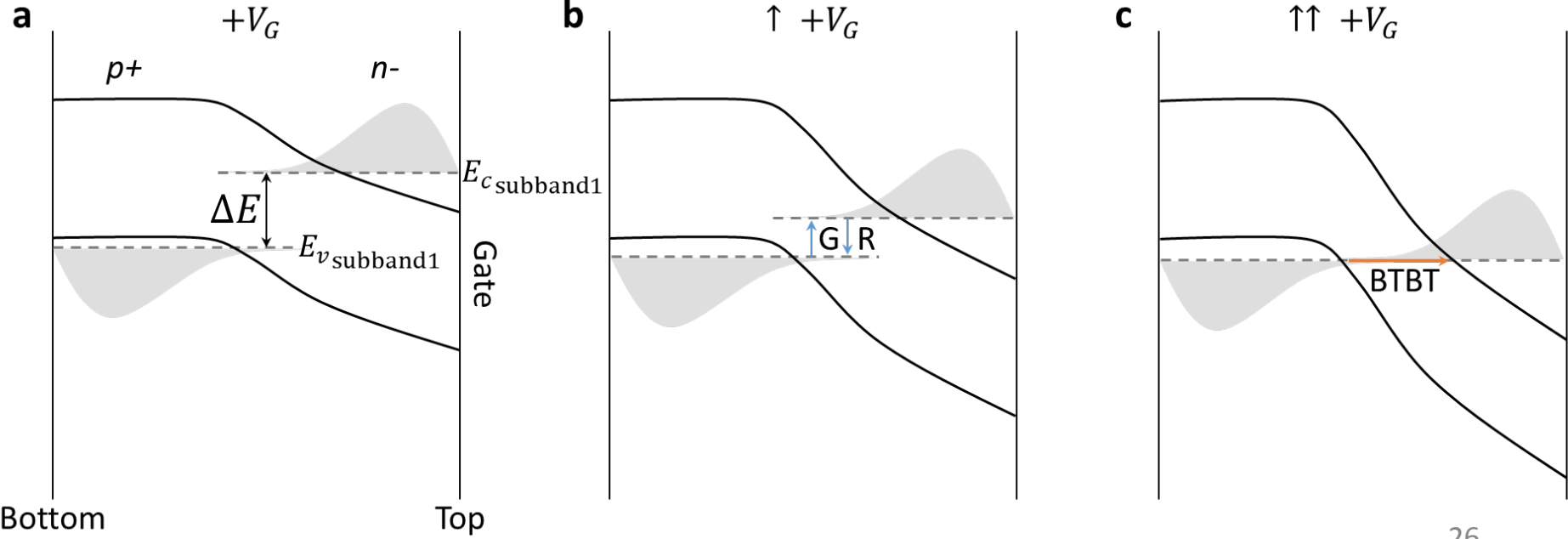
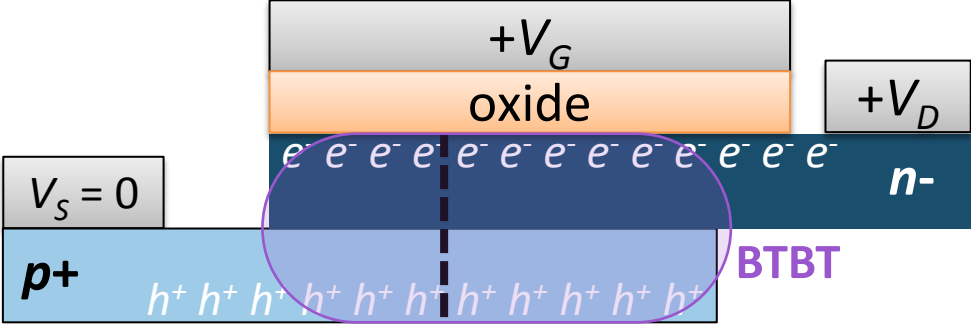
The concept is general and can be applied to other designs



# Band-to-band tunneling occurs vertically across the channel

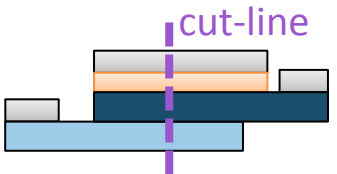
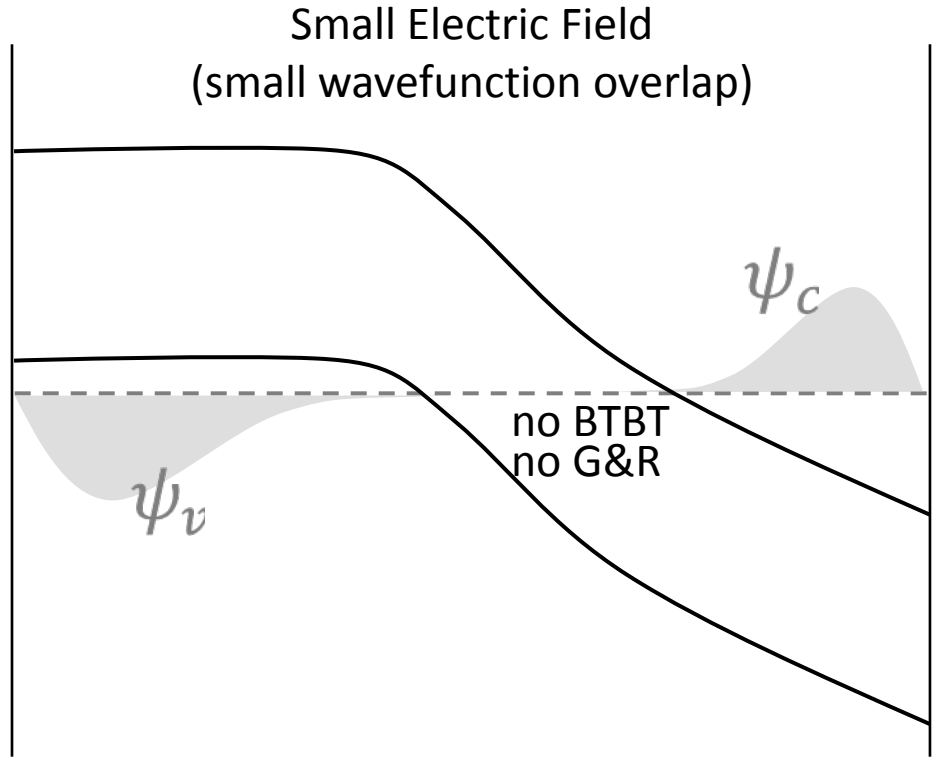
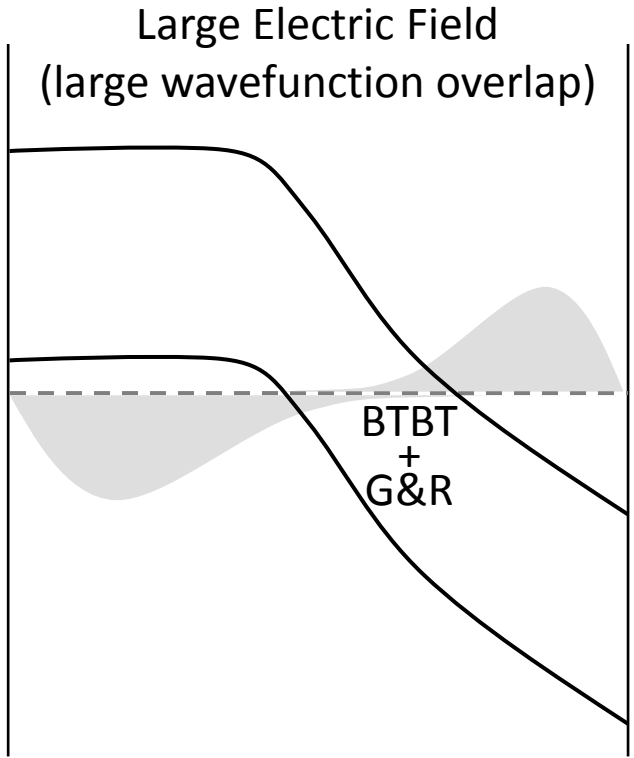


We turn the TFET on by  $\uparrow V_G$  to  $\downarrow \Delta E$



# BTBT and G&R are fundamentally linked through the wavefunction overlap

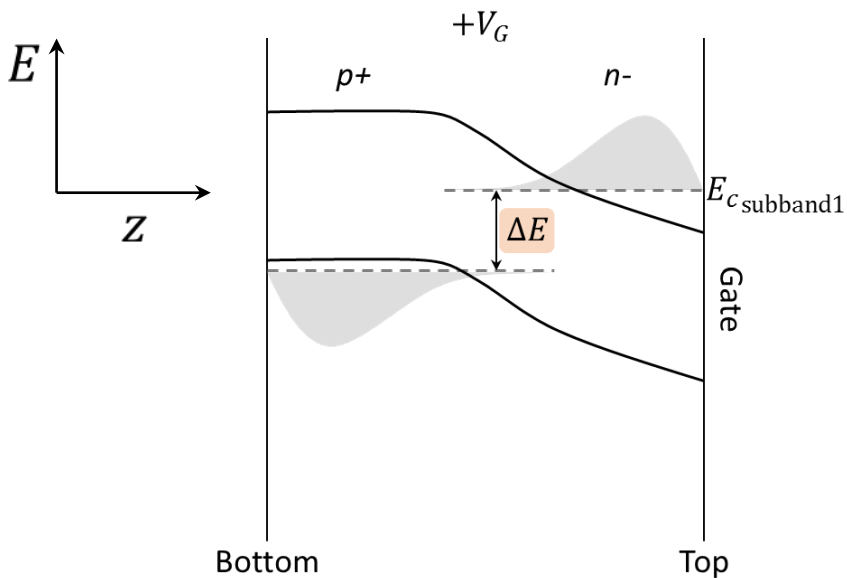
$$\langle \psi_v | \psi_c \rangle$$



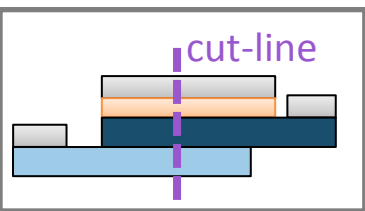
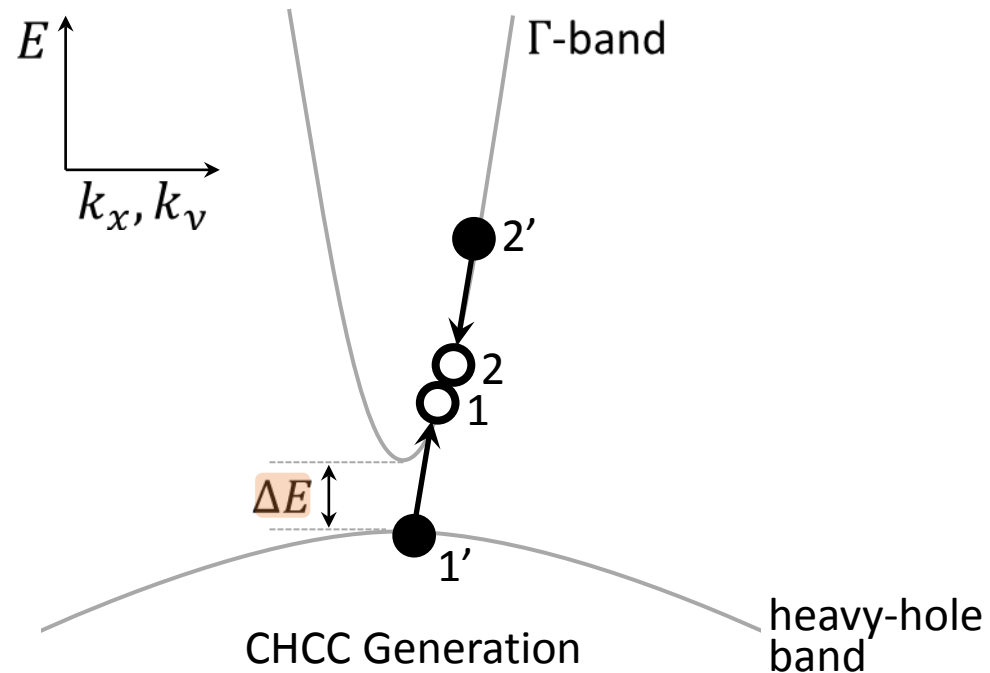
Proposed mechanism, **Auger generation** (also called impact ionization):

High-energy electron (2') knocks valence electron (1') into the conduction band

real space

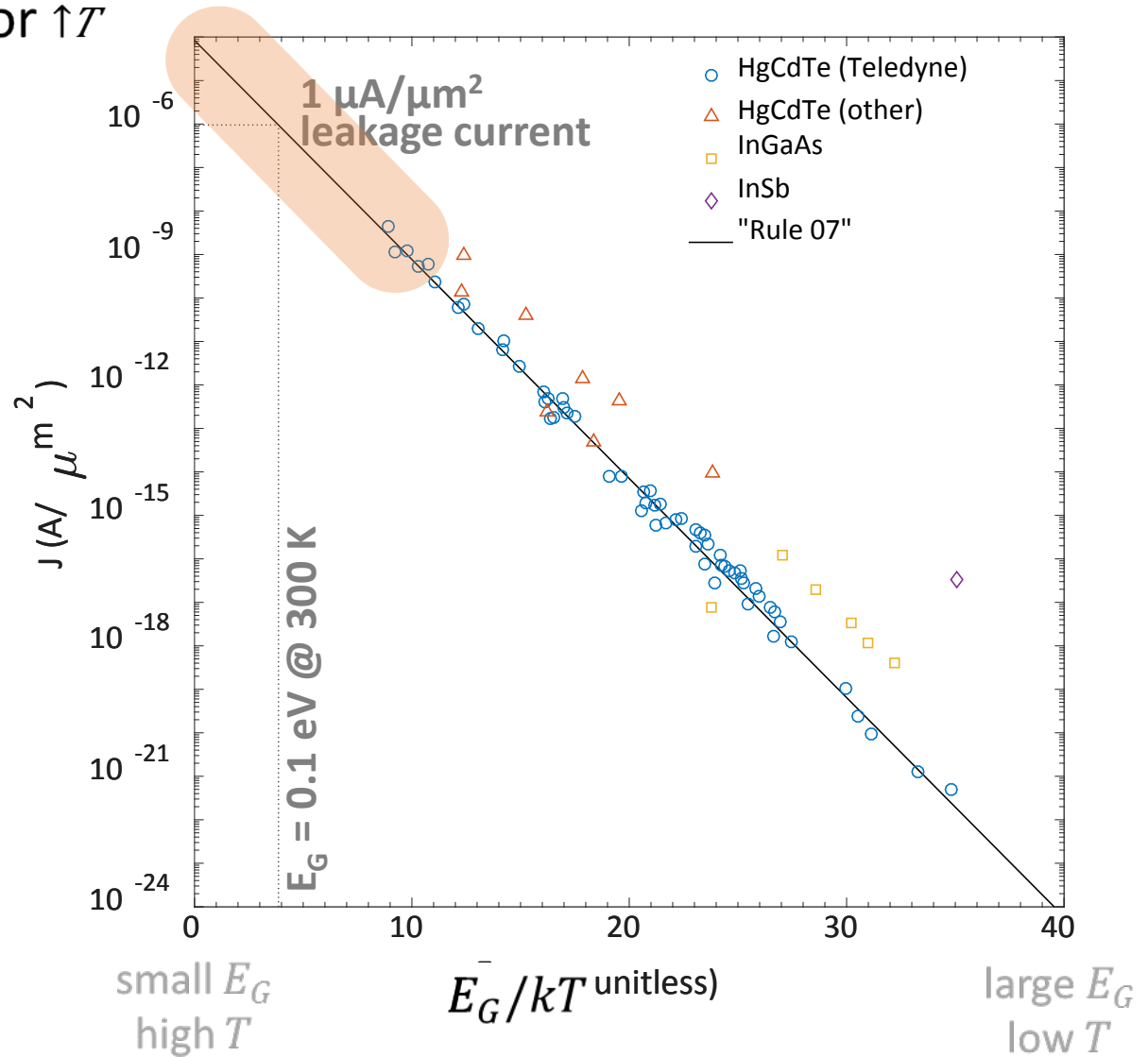


$k$ -space



# Auger leakage current in experimental photodectors

↑↑ Auger as ↓ $E_G$  or ↑ $T$

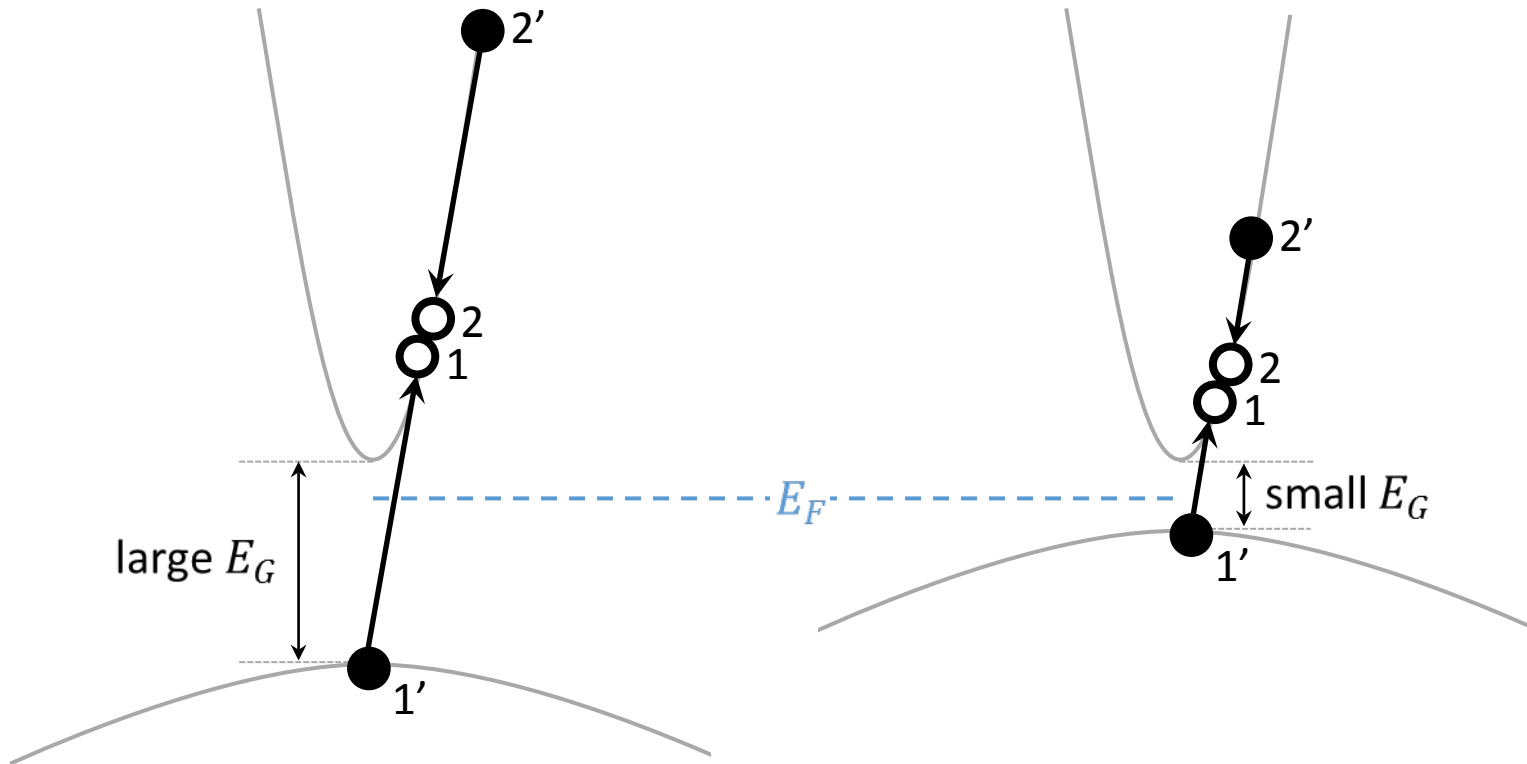


Tennant et al., "MBE HgCdTe Technology: A Very General Solution to IR Detection...", 2008.

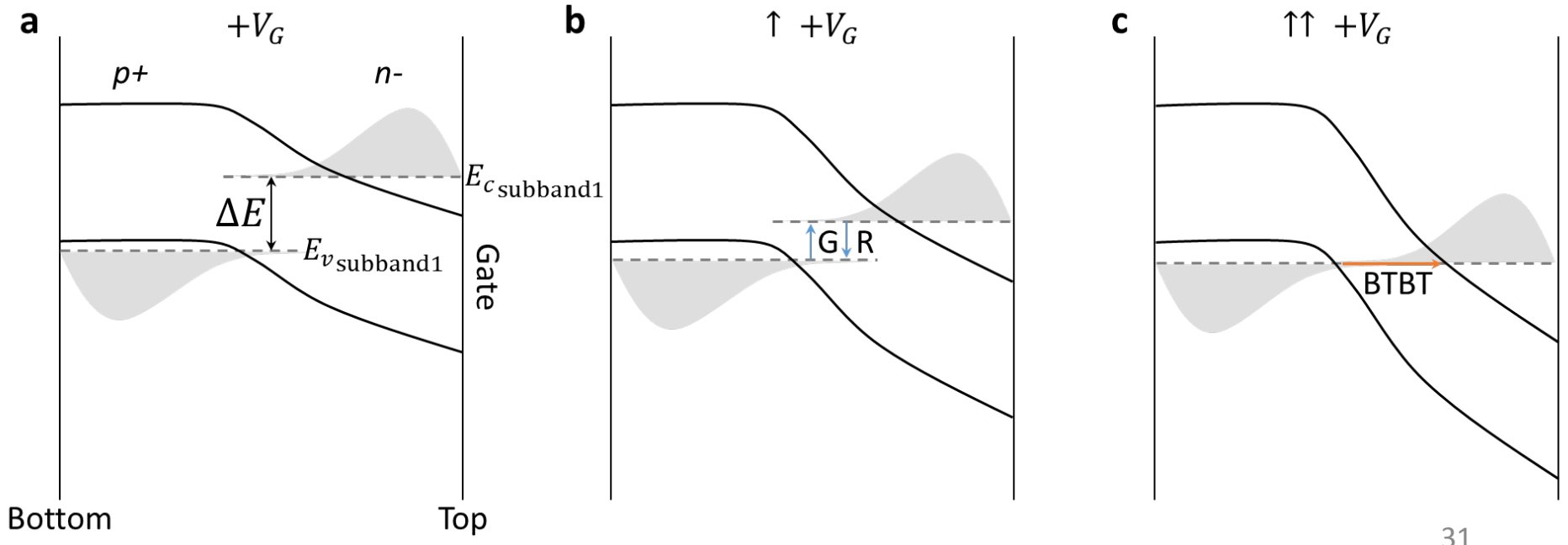
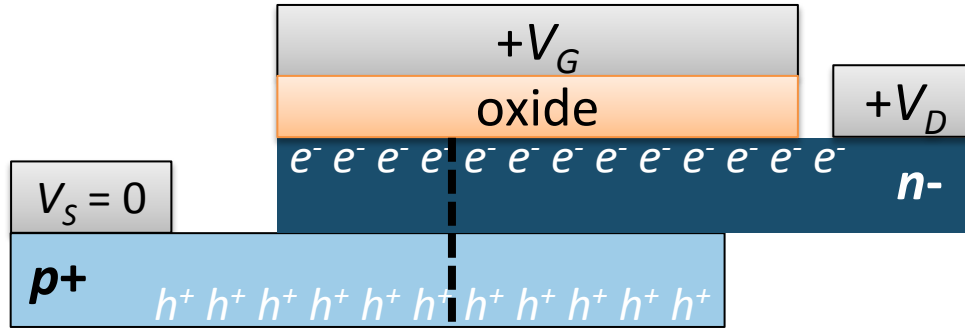
Tennant, "'Rule 07' Revisited: Still a Good Heuristic Predictor...", 2010.

To understand the photodiode results, review Auger transition

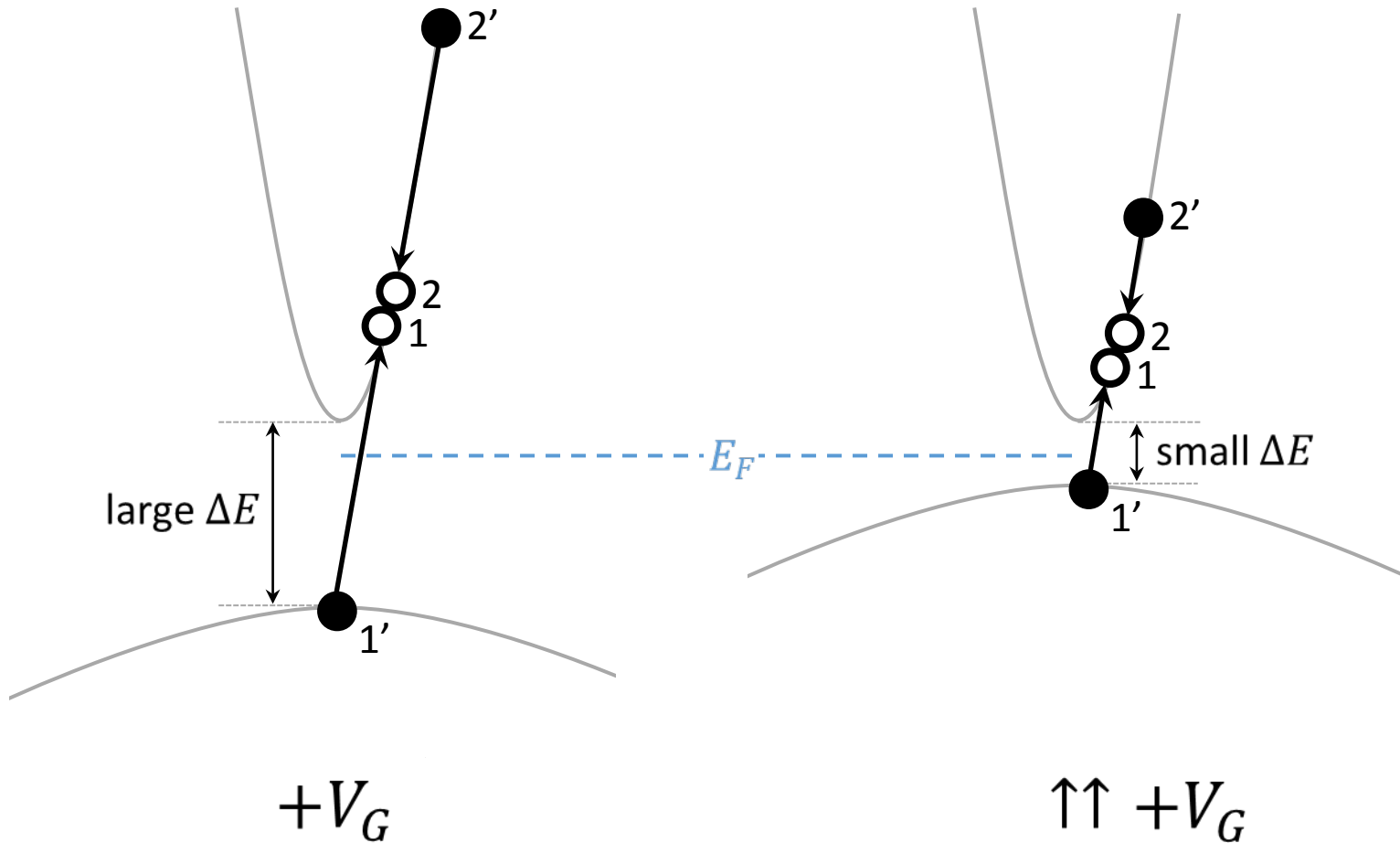
As  $\downarrow E_G$ , higher likelihood of *hot electron* with energy needed for generation



In TFET structure,  $\downarrow \Delta E$  instead of  $E_G$   
 $\uparrow\uparrow$  Auger as  $\downarrow \Delta E$



In TFET structure,  $\downarrow \Delta E$  instead of  $E_G$   
 $\uparrow\uparrow$  Auger as  $\downarrow \Delta E$

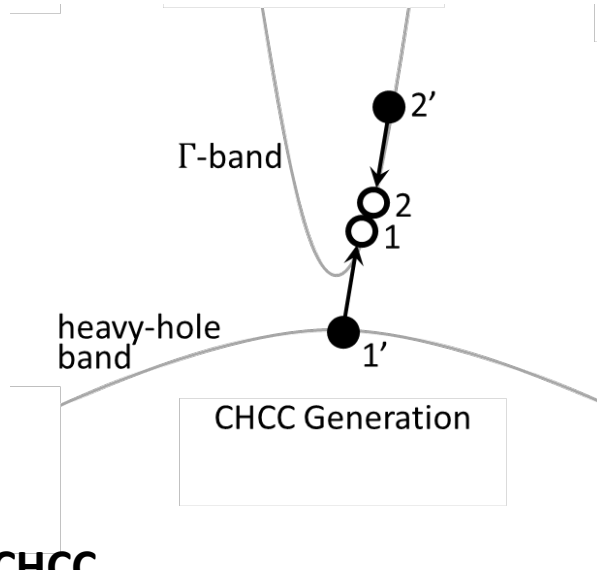




# Several types of Auger generation:

**CHCC** dominates for large electron concentrations

**HCHH** dominates for large hole concentrations

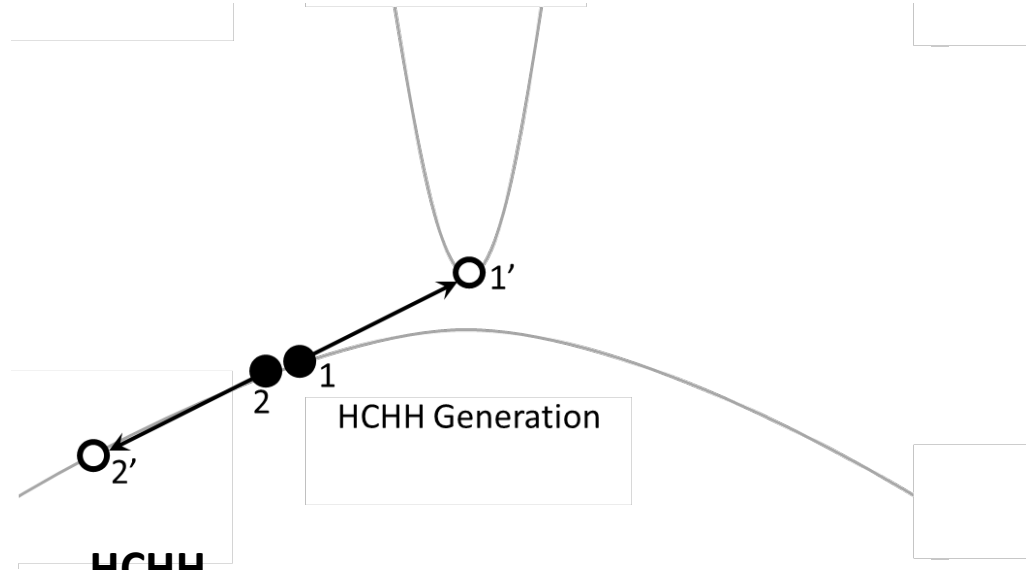


## CHCC

Dominant for large n-type doping

Dominant in **p-TFETs**

Depends on  $\mu = \frac{m_c}{m_v}$

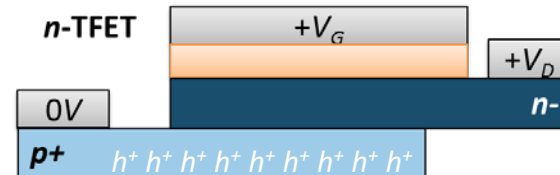
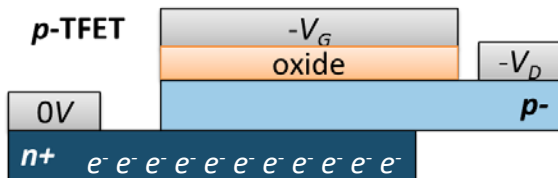


## HCHH

Dominant for large p-type doping

Dominant in **n-TFETs**

Depends on  $\mu^{-1} = m \downarrow v / m \downarrow c$



For CHCC, probability of an electron at  $E_{2'}$  limits gen. rate

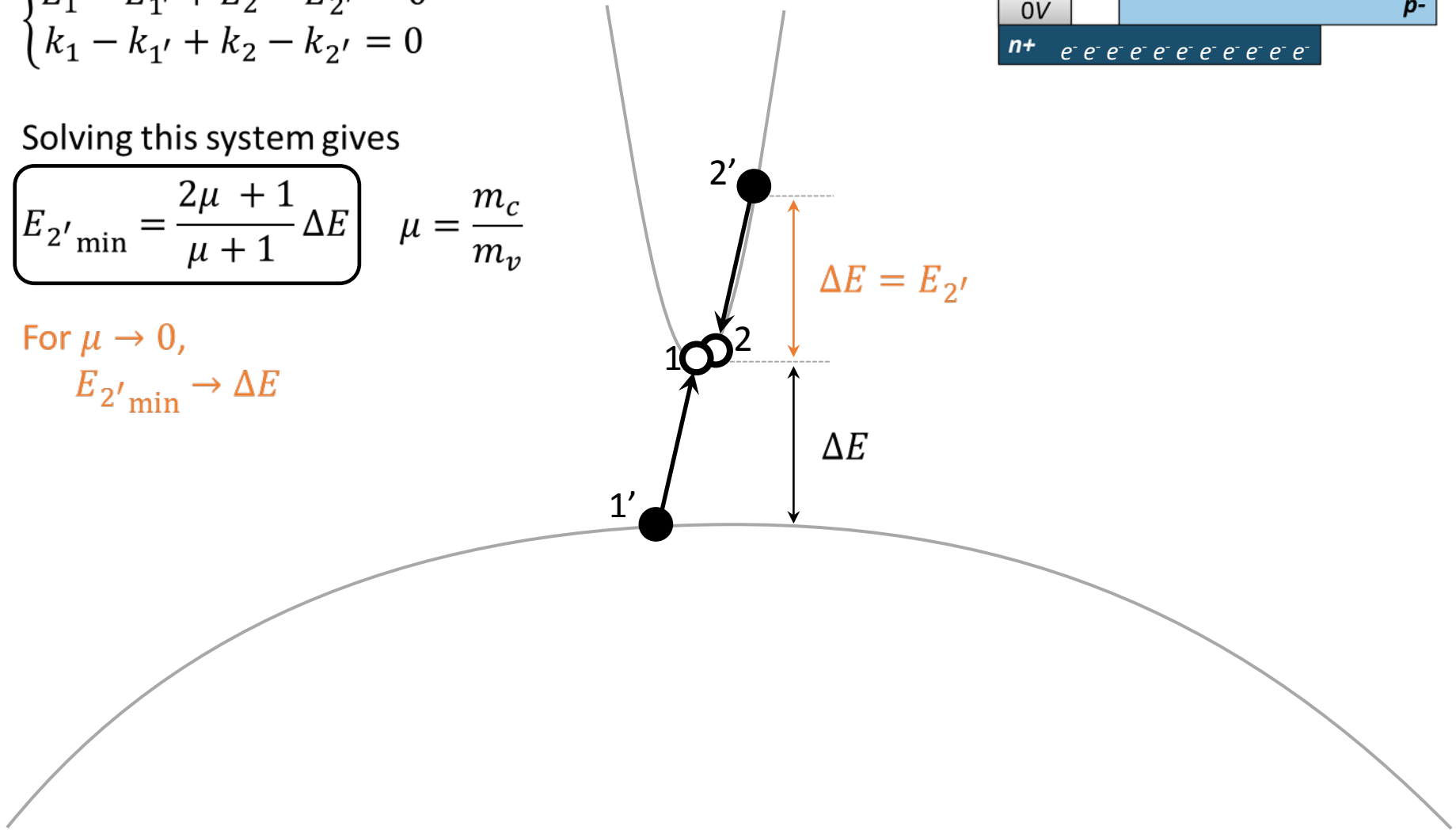
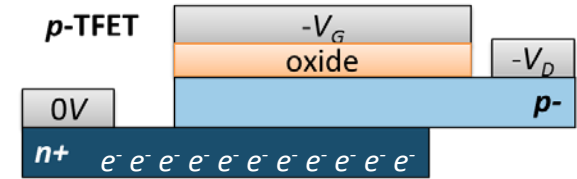
Energy and momentum conservation

$$\begin{cases} E_1 - E_{1'} + E_2 - E_{2'} = 0 \\ k_1 - k_{1'} + k_2 - k_{2'} = 0 \end{cases}$$

Solving this system gives

$$E_{2' \text{ min}} = \frac{2\mu + 1}{\mu + 1} \Delta E \quad \mu = \frac{m_c}{m_v}$$

For  $\mu \rightarrow 0$ ,  
 $E_{2' \text{ min}} \rightarrow \Delta E$



# For HCHH, probability of a hole at $E_{2'}$ limits gen. rate

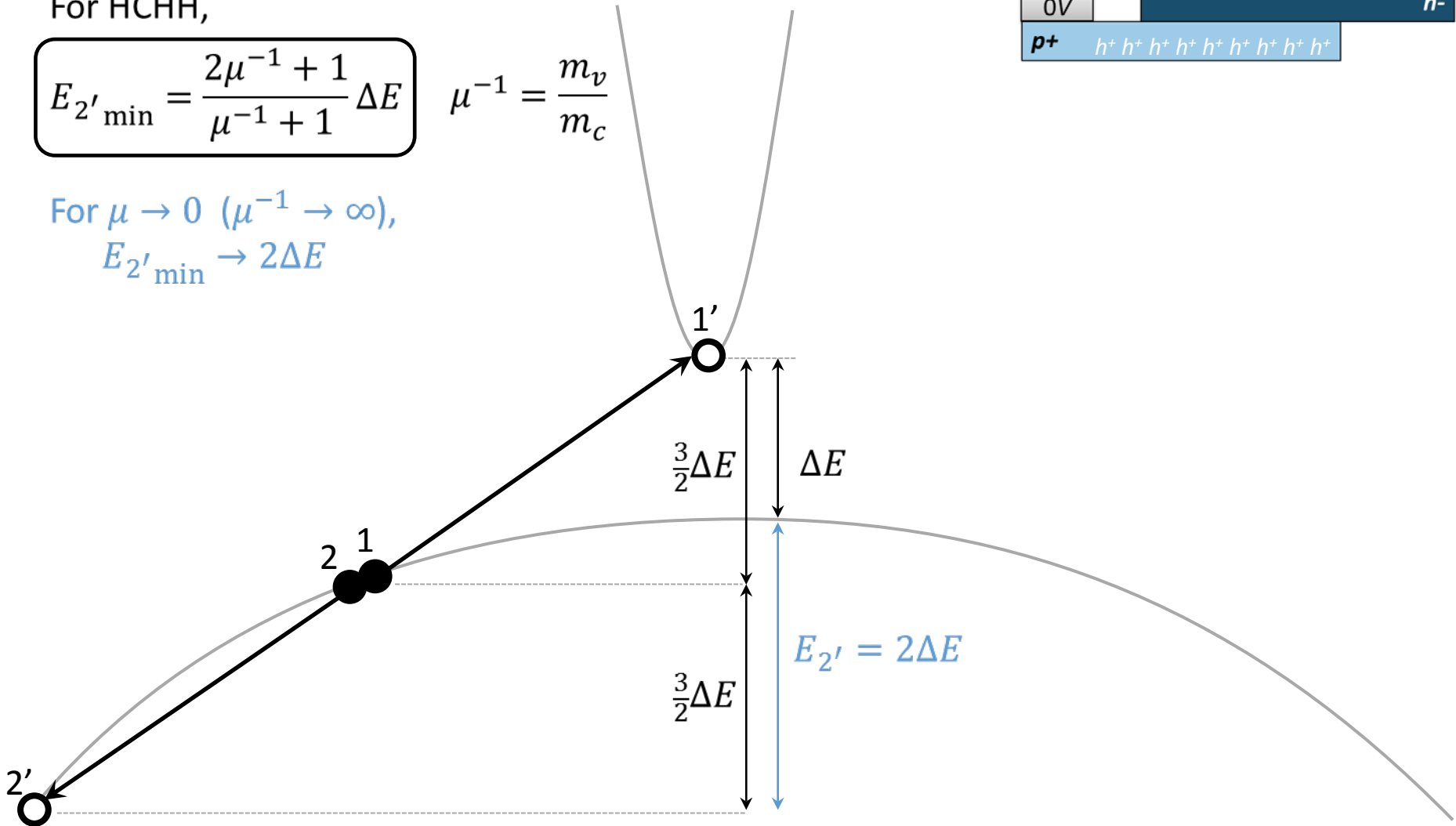
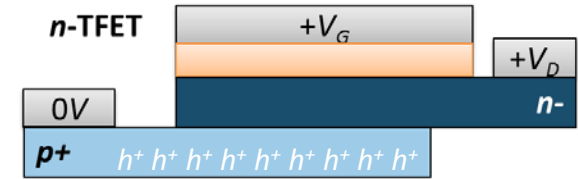
For HCHH,

$$E_{2' \min} = \frac{2\mu^{-1} + 1}{\mu^{-1} + 1} \Delta E$$

$$\mu^{-1} = \frac{m_v}{m_c}$$

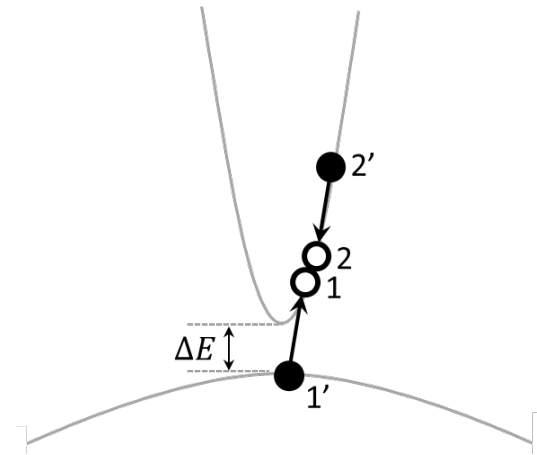
For  $\mu \rightarrow 0$  ( $\mu^{-1} \rightarrow \infty$ ),

$$E_{2' \min} \rightarrow 2\Delta E$$



# Net Auger transition rate is determined by Fermi's Golden Rule:

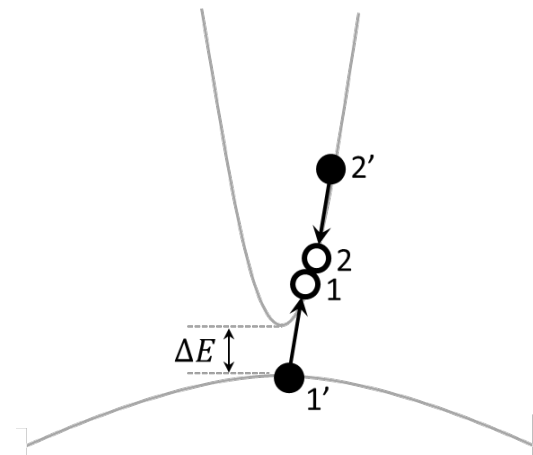
$$U = R - G = \frac{1}{A} \frac{2\pi}{\hbar} \sum_{1,1',2,2'} P(1,1',2,2') |M|^2 \delta(E_1 - E_{1'} + E_2 - E_{2'}) \left[ \frac{\# \text{ transition}}{\text{s} \cdot \text{cm}^2} \right]$$



# Counting all possible states:

Total rate is the sum of all the possible transitions

$$U = R - G = \frac{1}{A} \frac{2\pi}{\hbar} \sum_{1,1',2,2'} P(1,1',2,2') |M|^2 \delta(E_1 - E_{1'} + E_2 - E_{2'}) \left[ \frac{\# \text{ transition}}{\text{s} \cdot \text{cm}^2} \right]$$



# Probability of vacant/occupied states:

Weights the transition rate by the probability that particles needed for the transition are present

$$U = R - G = \frac{1}{A} \frac{2\pi}{\hbar} \sum_{1,1',2,2'} P(1,1',2,2') |M|^2 \delta(E_1 - E_{1'} + E_2 - E_{2'}) \left[ \frac{\# \text{ transition}}{s \cdot \text{cm}^2} \right]$$

For the transition pictured:

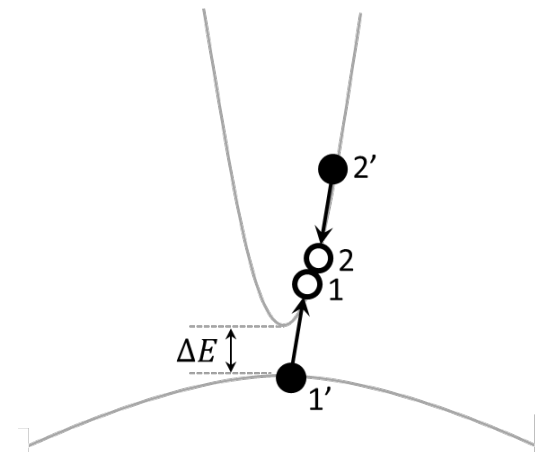
State 1 must be vacant

State 2 must be vacant

State 1' must be occupied

State 2' must be occupied

$$P = (1 - f_1)(1 - f_2)f_{1'}f_{2'} \\ \approx f_{2'}$$

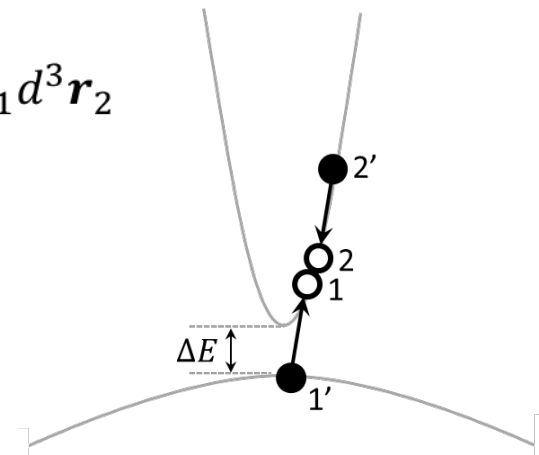


# Perturbation that causes the transition:

Coulomb interaction acting on the initial and final wavefunctions

$$U = R - G = \frac{1}{A} \frac{2\pi}{\hbar} \sum_{1,1',2,2'} P(1,1',2,2') |M|^2 \delta(E_1 - E_{1'} + E_2 - E_{2'}) \left[ \frac{\# \text{ transition}}{\text{s} \cdot \text{cm}^2} \right]$$

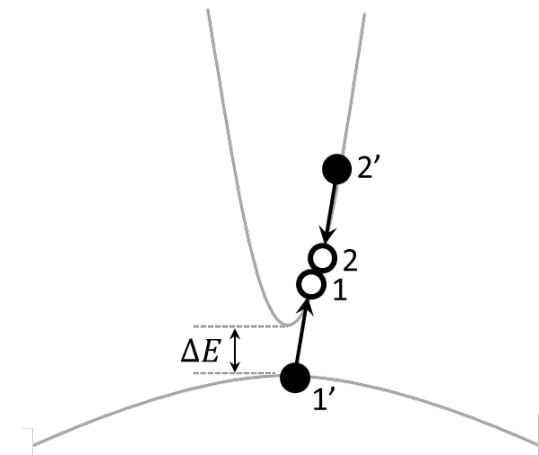
$$M = \iint \Psi_{1'}^*(\mathbf{r}_1) \Psi_{2'}^*(\mathbf{r}_2) \underbrace{\frac{q^2}{4\pi\epsilon|\mathbf{r}_1 - \mathbf{r}_2|}}_{\text{Coulombic potential}} \Psi_1(\mathbf{r}_1) \Psi_2(\mathbf{r}_2) d^3\mathbf{r}_1 d^3\mathbf{r}_2$$



# Conservation of energy:

We can't create or destroy energy in the transition

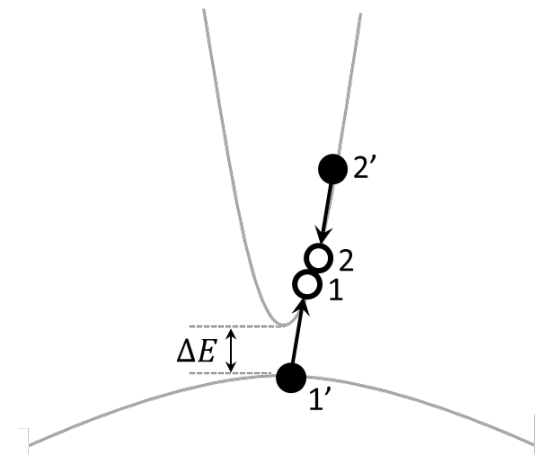
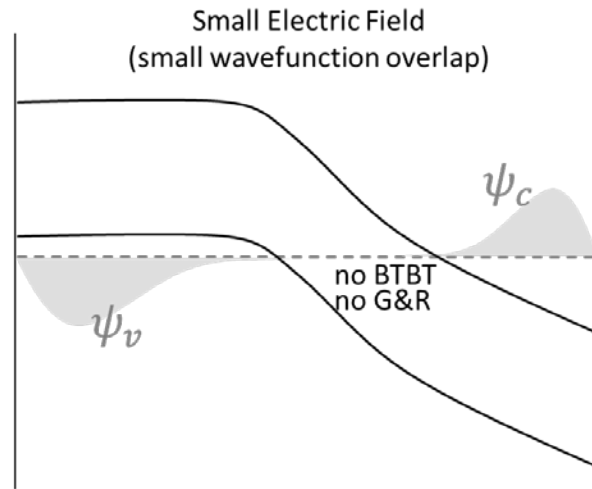
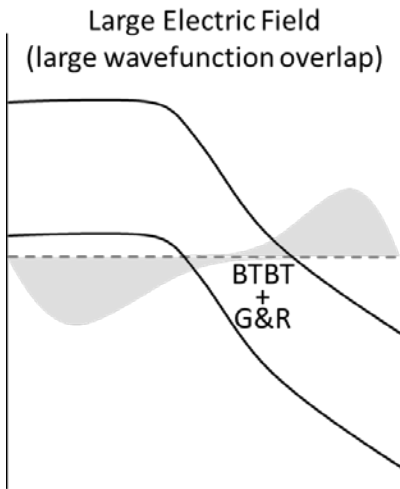
$$U = R - G = \frac{1}{A} \frac{2\pi}{\hbar} \sum_{1,1',2,2'} P(1,1',2,2') |M|^2 \delta(E_1 - E_{1'} + E_2 - E_{2'}) \left[ \frac{\# \text{ transition}}{\text{s} \cdot \text{cm}^2} \right]$$





After a lot of math (and a few approximations), we arrive at the generation rate per unit area

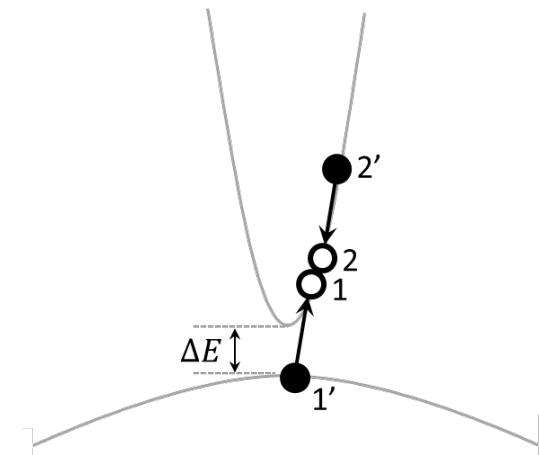
$$G_{CHCC} \approx \underbrace{\frac{q^4 m_c^3 (kT)^2 c_u^2}{4\pi^2 \hbar^7 \epsilon^2}}_{\text{Constants}} \underbrace{\frac{(\mu + 1)}{(2\mu + 1)^2} |\langle \psi_{1'} | \psi_1 \rangle|^2}_{\text{Wavefunction overlap}} \frac{n}{N_c} \exp\left(-\frac{(2\mu + 1) \Delta E}{(\mu + 1) kT}\right) \left[ \frac{\# \text{ transition}}{\text{s} \cdot \text{cm}^2} \right]$$



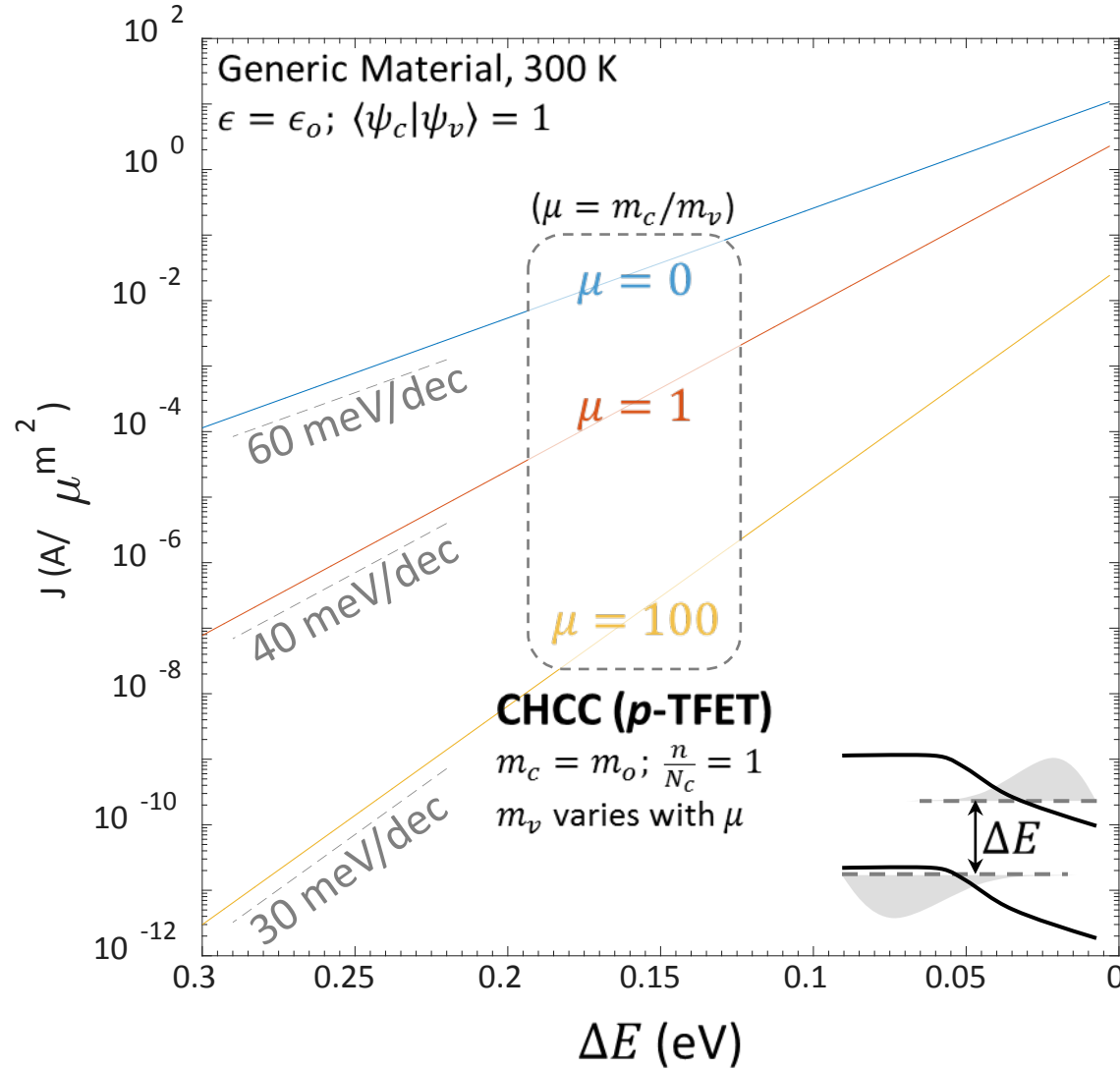
After a lot of math (and a few approximations),  
we arrive at the generation rate per unit area

$$G_{CHCC} \approx \underbrace{\frac{q^4 m_c^3 (kT)^2 c_u^2}{4\pi^2 \hbar^7 \epsilon^2}}_{\text{Constants}} \underbrace{\frac{(\mu + 1)}{(2\mu + 1)^2} |\langle \psi_{1'} | \psi_1 \rangle|^2}_{\text{Wavefunction overlap}} \overbrace{\frac{n}{N_c} \exp\left(-\frac{(2\mu + 1) \Delta E}{(\mu + 1) kT}\right)}^{\text{Probability of an electron at } E_{2'} \text{ min}} \left[ \frac{\# \text{ transition}}{\text{s} \cdot \text{cm}^2} \right]$$

$E_{2'} \text{ min}$

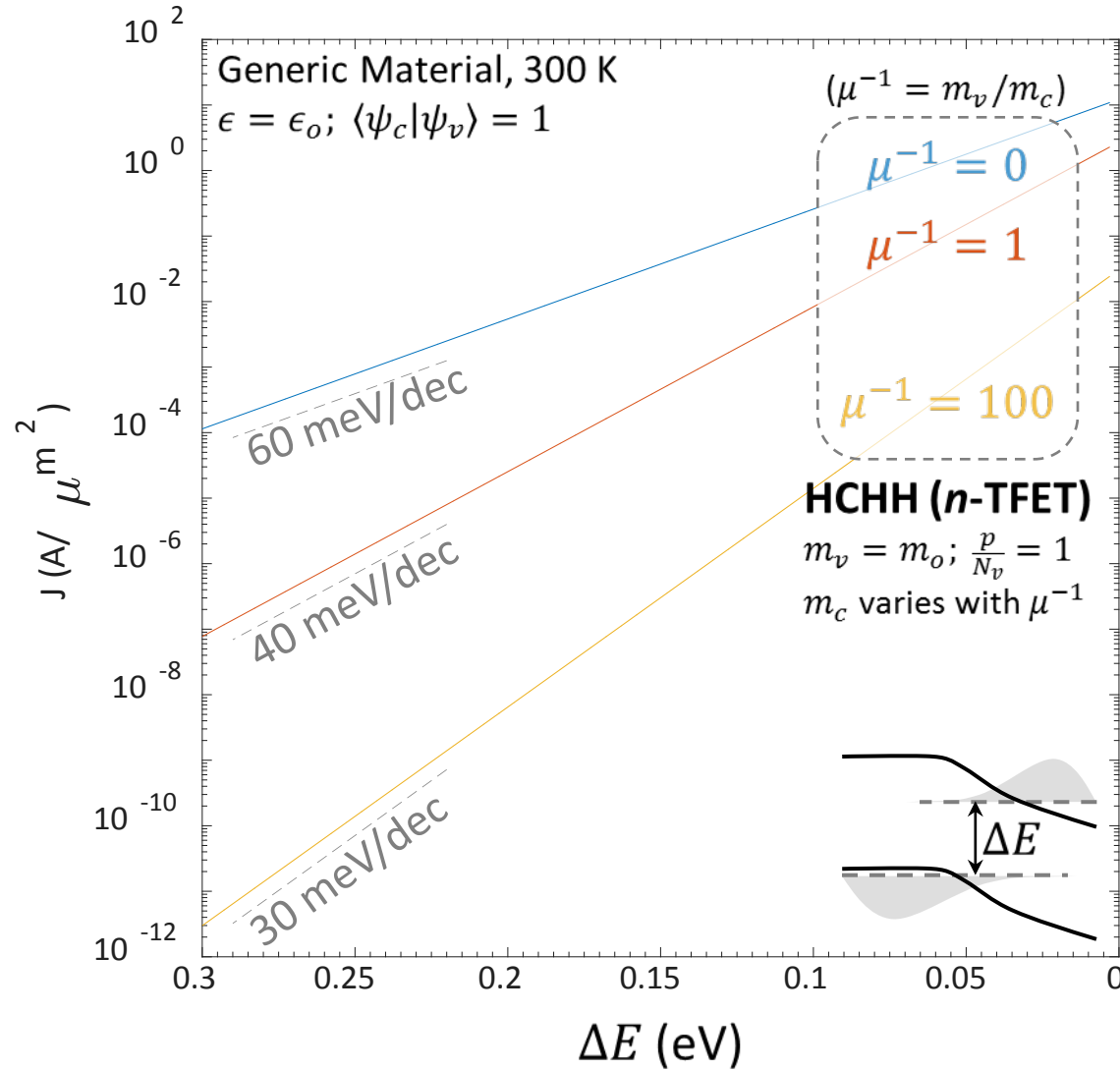


# Auger current density calculated from the generation rate



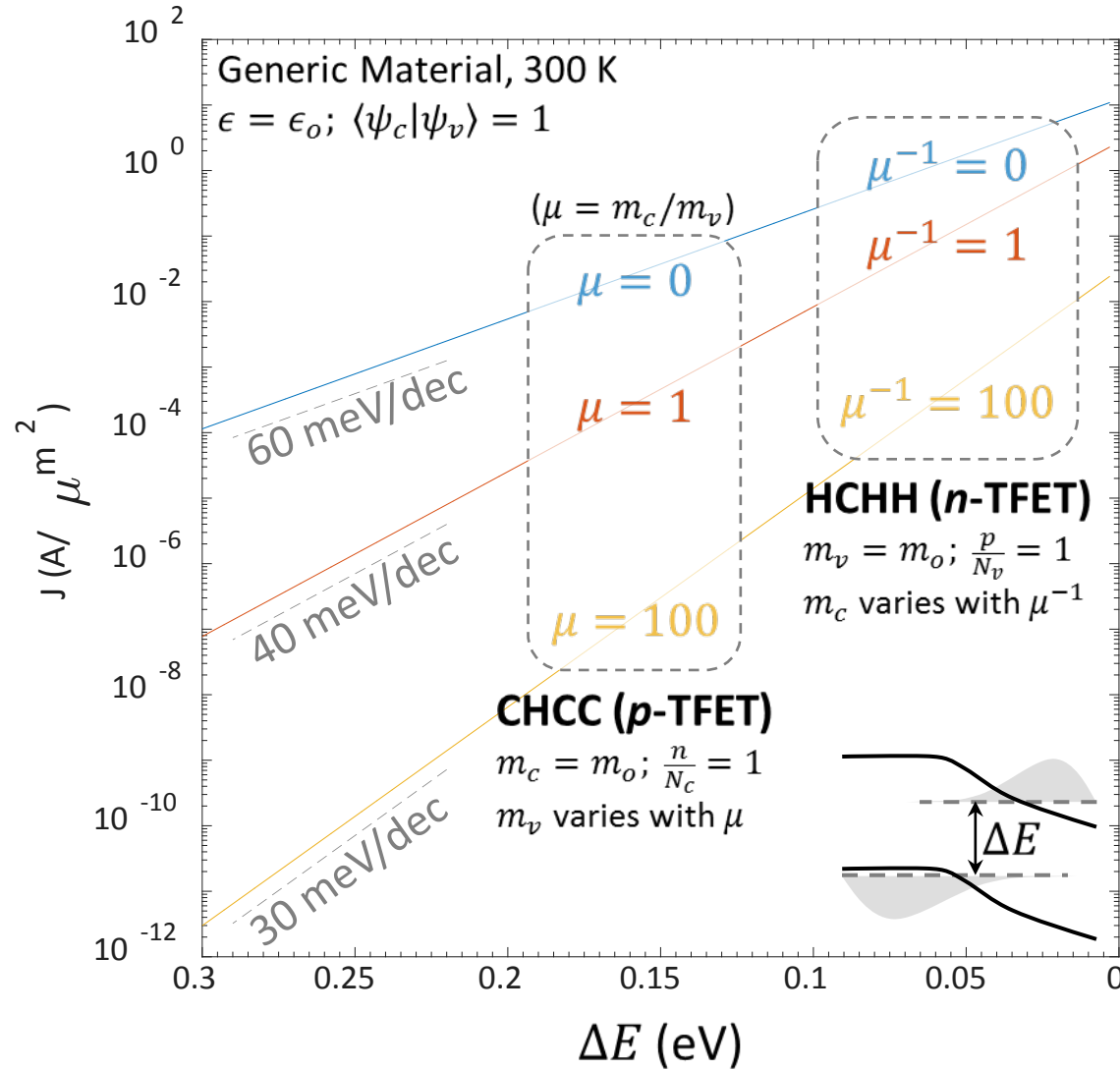
$$J = qG_{CHCC} \approx \frac{q^4 m_c^3 (kT)^2 c_u^2}{4\pi^2 \hbar^7 \epsilon^2} \frac{(\mu + 1)}{(2\mu + 1)^2} |\langle \psi_{1'} | \psi_1 \rangle|^2 \frac{n}{N_c} \exp\left(-\frac{(2\mu + 1) \Delta E}{(\mu + 1) kT}\right)$$

# Auger current density calculated from the generation rate



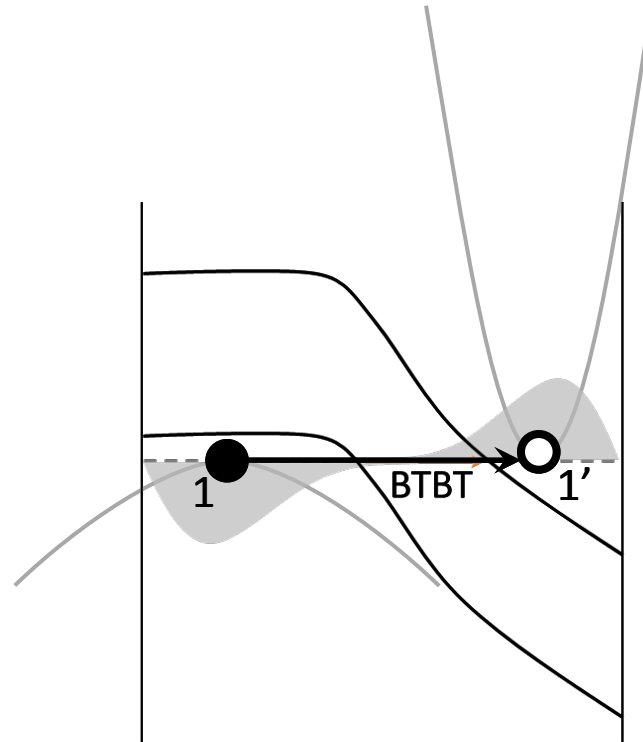
$$J = qG_{HCHH} \approx \frac{q^4 m_v^3 (kT)^2 c_u^2}{4\pi^2 \hbar^7 \epsilon^2} \frac{(\mu^{-1} + 1)}{(2\mu^{-1} + 1)^2} |\langle \psi_{1'} | \psi_1 \rangle|^2 \frac{p}{N_v} \exp\left(-\frac{(2\mu^{-1} + 1) \Delta E}{(\mu^{-1} + 1) kT}\right)$$

# Auger current density calculated from the generation rate



$$J = qG_{CHCC} \approx \frac{q^4 m_c^3 (kT)^2 c_u^2}{4\pi^2 \hbar^7 \epsilon^2} \frac{(\mu + 1)}{(2\mu + 1)^2} |\langle \psi_{1'} | \psi_1 \rangle|^2 \frac{n}{N_c} \exp\left(-\frac{(2\mu + 1) \Delta E}{(\mu + 1) kT}\right)$$

# Visualization of band-to-band tunneling in terms of energy band diagram and $E-k$ diagram



Ideal band-to-band tunneling can only take place when  $\Delta E = 0$

# Band-to-band tunneling has key similarities to Auger

- Both can be viewed as generation and recombination events
- Fermi's Golden Rule can be used to calculate transition rate

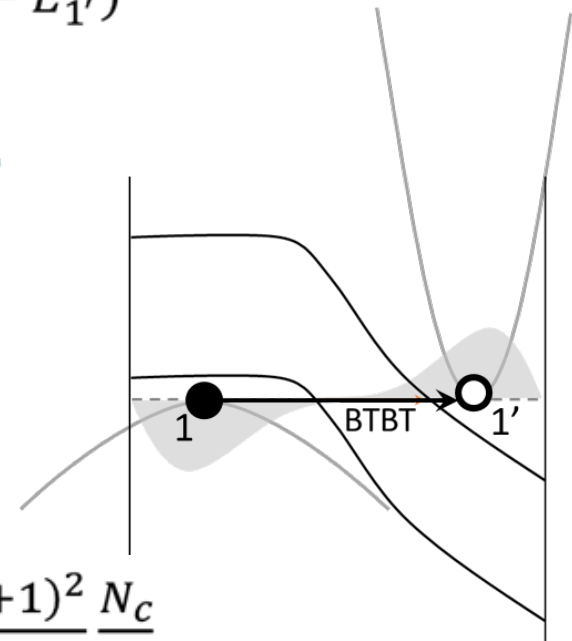
- $U_{Auger} = R - G = \frac{1}{A} \frac{2\pi}{\hbar} \sum_{1,1',2,2'} P(1, 1', 2, 2') |M|^2 \delta(E_1 - E_{1'} + E_2 - E_{2'})$

- $U_{BTBT} = R - G = \frac{1}{A} \frac{2\pi}{\hbar} \sum_{1,1'} P(1, 1') |M|^2 \delta(E_1 - E_{1'})$

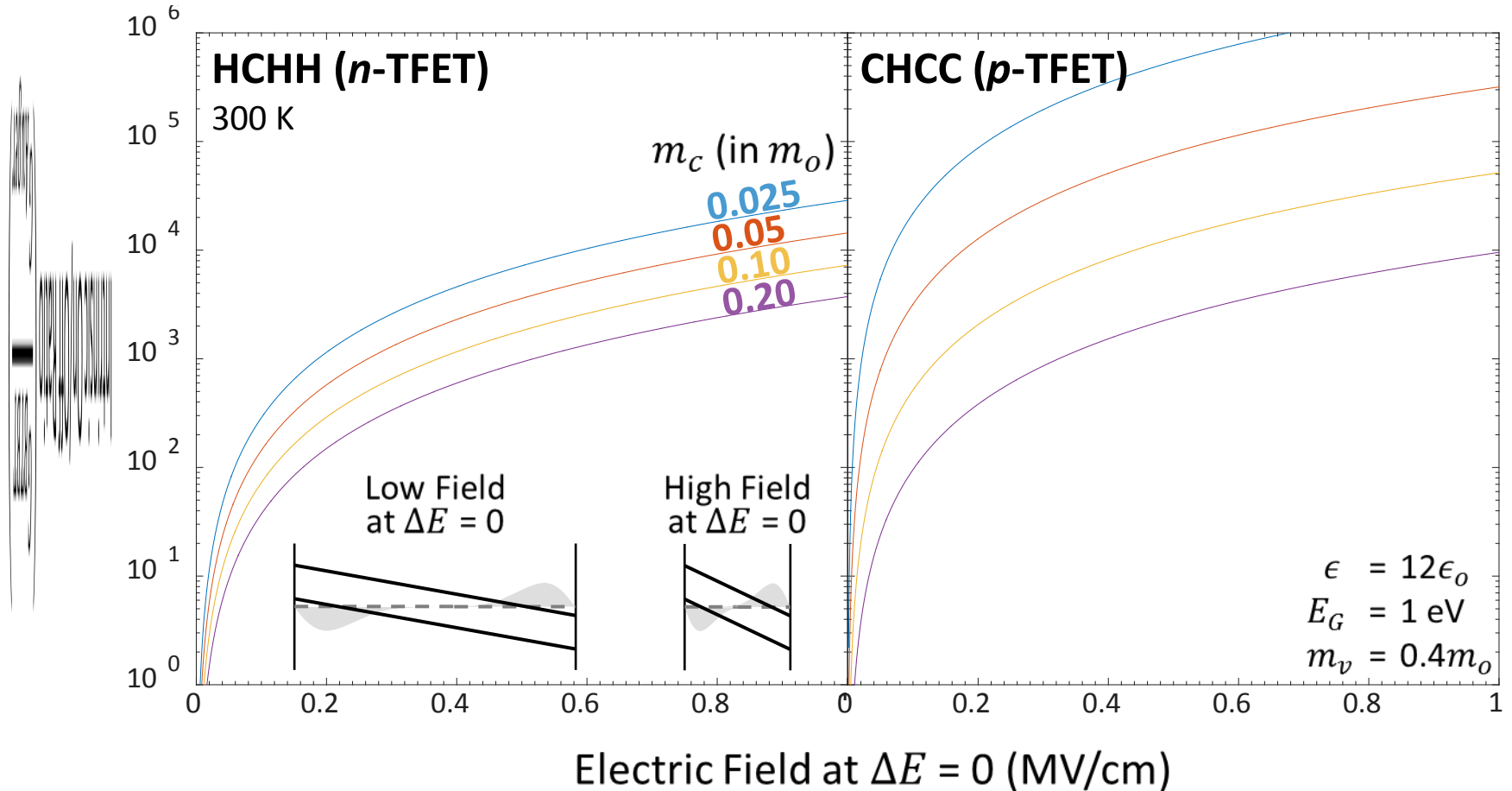
- $M_{Auger} = \frac{q^2}{2\epsilon A} c_u \delta_{\mathbf{k}_{\perp 1} - \mathbf{k}_{\perp 1'} + \mathbf{k}_{\perp 2} - \mathbf{k}_{\perp 2'}} \langle \psi_{1'} | \psi_1 \rangle$

- $M_{BTBT} = \int \Psi_{1'}^*(\mathbf{r}) q\phi(z) \Psi_1(\mathbf{r}) d^3\mathbf{r}$   
 $= (qF) z_{cv} \delta_{\mathbf{k}_{\perp 1} - \mathbf{k}_{\perp 1'}} \langle \psi_{1'} | \psi_1 \rangle$

- At  $\Delta E = 0$ :  $\frac{G_{BTBT}}{G_{CHCC}} = \frac{(qF)^2}{E_G} \frac{2\pi^2 \hbar^6 \epsilon^2}{q^4 m_c^3 (kT)^2 c_u^2} \frac{(2\mu+1)^2 N_c}{(\mu+1) n}$



# Intrinsic on/off ratio (at turn-on) for TFETs due to Auger generation



At  $\Delta E = 0$ :

$$\frac{G_{BTBT}}{G_{CHCC}} = \frac{(qF)^2}{E_G} \frac{2\pi^2 \hbar^6 \epsilon^2}{q^4 m_c^3 (kT)^2 c_u^2} \frac{(2\mu+1)^2 N_c}{(\mu+1) n}$$



# Some remarks

Auger is intrinsic, no easy way to reduce it

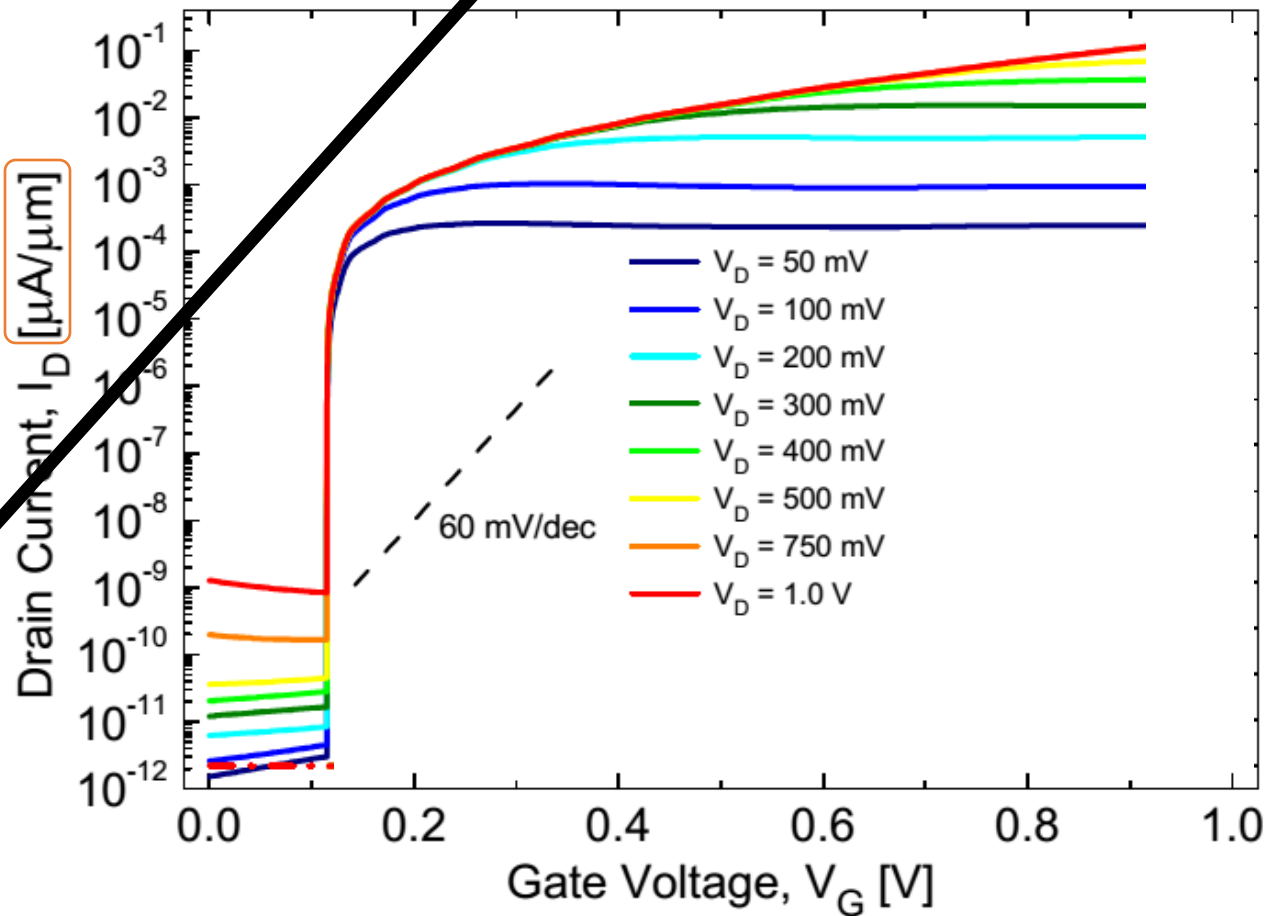
- Decreasing doping decreases Auger, but also reduces field and hence BTBT
- Problematic for steep slope device because of Arrhenius dependence on  $\Delta E$

Auger and BTBT are both *generation* phenomena, and are tightly linked

- Decreasing Auger likely decreases BTBT as well

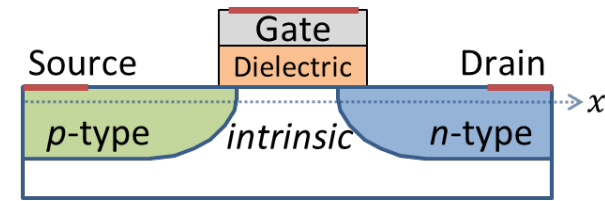
# Simulated band-to-band tunneling current for a bilayer TFET

Auger current

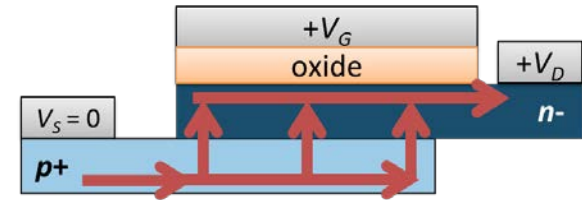


# Future Work

- Extending the analysis to different device geometries
  - Point TFET
- Experimental verification of Auger phenomenon
  - Vary doping with electrostatic gating
- Demonstration of an Auger FET with sub-60 mV/decade SS



**Point TFET**



**Perpendicular TFET**

# Summary

- Experimental TFETs have not lived up to *ideal* simulations
- We need to understand the reasons for the discrepancies
- Auger can be especially problematic for small  $E_G$  or  $\Delta E$ 
  - leads to significant off-state currents that may dictate subthreshold behavior
- Future TFET work must include non-ideal effects such as Auger